Journal of Environmental Radioactivity 289 (2025) 107751

Contents lists available at ScienceDirect

Journal of Environmental Radioactivity

journal homepage: www.elsevier.com/locate/jenvrad

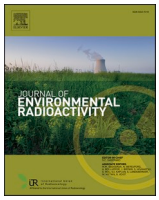

Parameter uncertainty analysis of the committed equivalent dose coefficients from inhalation of radon progeny in underground uranium mines

Thomas Makumbi [a,*], Bastian Breustedt [b], Wolfgang Raskob [a], Sadeeb Simon Ottenburger [a]

[a] Institute for Thermal Energy Technology and Safety (ITES), Karlsruhe Institute of Technology (KIT), Hermann-von-Helmholtz Platz 1, 76344, Eggenstein-Leopoldshafen, Germany
[b] Institute of Biomedical Engineering (IBT), Karlsruhe Institute of Technology (KIT), Kaiserstraße 12, 76131, Karlsruhe, Germany

ARTICLE INFO

Keywords:
Radon progeny
Committed equivalent dose coefficient
Uncertainty analysis
Sensitivity analysis
Underground mines

ABSTRACT

This study evaluates the uncertainties in committed equivalent dose coefficients from inhalation of radon progeny in underground uranium mines. The work focuses on two exposure scenarios: wet drilling with good ventilation (Job 1) and dry drilling with poor ventilation (Job 4). The use of Monte Carlo simulations informed by the International Commission on Radiological Protection (ICRP) latest biokinetic models and parameter probability distributions obtained from published literature, revealed that Job 4 conditions yield higher lung dose coefficients than Job 1, despite both scenarios exhibiting similar uncertainty levels. The committed equivalent lung dose coefficients followed lognormal distributions, with geometric means of 61.87 mSv/(mJh/m^3) and geometric standard deviation of 1.56 for Job 4 and 47.05 mSv/(mJh/m^3) and geometric standard deviation of 1.58 for Job 1. The alveolar-interstitial region showed the greatest uncertainty, while the bronchial secretory cells received the highest doses. Among systemic organs, the kidneys received the largest dose. Statistical tests confirmed significant differences between the two job types. Sensitivity analysis identified tidal volume as main contributor to committed equivalent lung dose coefficient uncertainty. These findings support revising model parameters and improving breathing parameter measurements to enhance dose accuracy. The study emphasizes the necessity for enhanced ventilation, stricter air quality standards, and advanced personal protective equipment to mitigate health risks in radon-prone mining environments.

1. Introduction

Radon progeny poses significant radiation exposure risks that require effective protection strategies based on sound science and societal considerations. The RadoNorm project radonorm, (https://www.radonorm.eu) was initiated to address these concerns by improving risk management approaches for radon and NORM exposure situations. As part of this initiative, Task 3.4 focused on the assessment of uncertainties affecting dose distribution in cohort studies, with the aim of refining the uncertainties affecting the dose-response relationship. Specifically, this task examined how variations in model parameters affect dose calculations for selected human organs and tissues (https://www.radonorm.eu/workpackages/wp3-tasks/).

Epidemiological studies have shown that inhalation of radon gas and its progeny is a major cause of lung cancer, particularly among underground miners and indoor workers (Hu et al., 2020; Chen, 2023; Skubacz et al., 2023). The lung is the organ that receives the highest dose, with approximately 95 % of this dose attributable to the inhalation of radon progeny rather than the gas itself (Marsh et al., 2008, 2012). This is because almost all inhaled radon gas is exhaled, whereas its short-lived progeny deposit in the respiratory tract and deliver a significant dose before being cleared either by absorption into the blood or by particle transport to the alimentary tract (Papenfuβ et al., 2023).

Two major short-lived radon progeny, Po-218 and Po-214, decay by alpha emission. The energy released by these alpha particles accounts for most of the radiation dose to the lung tissue (Romano et al., 2019). Equivalent dose coefficients to body organs and tissues following inhalation of radon progeny can be estimated using biokinetic models developed by the International Commission for Radiological Protection (ICRP). However, a major challenge in the assessment of committed

* Corresponding author.
E-mail address: thomas.makumbi@kit.edu (T. Makumbi).

https://doi.org/10.1016/j.jenvrad.2025.107751
Received 16 March 2025; Received in revised form 25 May 2025; Accepted 1 July 2025
Available online 5 July 2025

equivalent dose coefficients to organs and tissues is that the ICRP models are reference models with parameter values based on a standardized reference person. By definition, these models use fixed parameter values without associated uncertainties (Paquet et al., 2016). Therefore, sensitivity analysis and uncertainty estimation of key parameters in these models is essential to improve model understanding and to assess the impact of parameter variations on dose predictions (Breustedt et al., 2017, 2018).

Previous studies have evaluated the impact of model parameter uncertainties on lung dose calculations following inhalation of radon progeny in underground mining environments. One notable study by Marsh and Birchall (2009) performed an uncertainty analysis of the absorbed dose per unit exposure using the ICRP 66 lung model (ICRP, 1994). However, their study was based on an older dosimetric framework and did not incorporate the most recent ICRP Occupational Intake of Radionuclides (OIR) models (ICRP, 2006, 2015; 2017). In addition, the exposure scenarios of Marsh and Birchall (2009), differed from those considered in the present study, as they investigated wet drilling with medium ventilation (Job 2) as well as wet drilling with good ventilation and diesel engines (Job 0).

Unlike previous studies, the present study focuses on two specific occupational exposure scenarios i.e., wet drilling with good ventilation (Job 1) and dry drilling with poor ventilation (Job 4). This focus was driven by the objectives of the RadoNorm project, in which epidemiologists sought to evaluate the impact of uncertainties in model parameters on the calculation of dose coefficients employed in cohort studies of former uranium miners at the Wismut Company in East Germany between 1946 and 2003 (Kreuzer et al., 2002, 2008, 2010; Grosche et al., 2006).

Uranium mining by the Wismut Company, particularly between 1946 and 1989, underwent several distinct operational phases. From 1946 to 1954, mining conditions were characterized by dry drilling techniques, lack of forced ventilation and consequently elevated exposure to radon (Kreuzer et al., 2002, 2010), conditions representative of Job 4. In contrast, the period from 1955 to 1970 saw substantial improvements in occupational safety, including the adoption of wet drilling methods and enhanced ventilation systems (Kreuzer et al., 2002, 2010; Grosche et al., 2006). These improvements resulted in significantly lower radon levels and reduced dust exposure, which are characteristic of Job 1.

Following the implementation of various international radiation protection and occupational safety standards after 1970, such as the introduction of individual radon exposure monitoring, there was a significant shift in occupational health practices in the uranium mining sector (Grosche et al., 2006). These regulatory advancements emphasized the importance of evaluating the impact of these measures on miners' health outcomes. Consequently, it became important to calculate and compare reference dose coefficients, along with the associated uncertainties, under two representative exposure conditions i.e. Job 1 and Job 4. Readers are referred to an earlier publication by the authors (Makumbi et al., 2024a) for a detailed discussion of the aerosol properties characterizing these two exposure scenarios.

This study focused on uncertainties arising from exposure scenarios and biokinetic parameters of radon progeny, excluding those arising from the dosimetric model. This is because the dosimetric model relies on well-established nuclear decay data and fixed radiation weighting factors published by the ICRP. Alpha particles, which are the main contributors to dose, are fully absorbed in source regions. Therefore, uncertainties in dosimetric parameters, such as the specific absorbed fraction (SAF), were considered negligible (Makumbi et al., 2024a). Unlike Marsh and Birchall (2009), who included dosimetric uncertainties but omitted radiation and tissue weighting factors, this study evaluates the effect of uncertainty in exposure and biokinetics on organ and tissue dose coefficients relevant to the RadoNorm project.

A key distinction of the present work is the estimation of committed equivalent dose coefficients rather than absorbed doses. Additionally, this study applies the latest ICRP models, which provide a more physiologically and biologically realistic representation of human body processes. Thus, its results contribute to a more comprehensive understanding of uncertainty in dose assessment, ultimately supporting more effective radiation protection strategies for radon progeny exposure scenarios.

This study built on previous research conducted by the authors on uncertainty and sensitivity analyses of committed equivalent dose coefficients. These earlier investigations involved a review of the parameters affecting the committed equivalent lung dose coefficient following inhalation of radon progeny in underground mines, together with their associated probability distributions (Makumbi et al., 2024a). In addition, the authors developed an in-house software tool to implement the ICRP internal dose assessment methodology and to perform uncertainty and sensitivity studies on calculated dose values (Breustedt et al., 2024; Makumbi et al., 2024b).

Building on these foundations, the study used prior distributions of biokinetic model parameters and other exposure scenario parameters relevant to radon progeny intake in underground mines identified in the earlier study by the authors (Makumbi et al., 2024a). Additionally, the in-house developed software tool, INTDOSKIT, was also used to quantify uncertainties in the calculated committed equivalent dose coefficients. Hence, by integrating these outputs, this study improves the robustness of dose assessments for occupational exposure to radon progeny in underground mines.

2. Description of job types in underground uranium mining

Underground mining involves several subsurface techniques aimed at efficiently extracting mineral resources (Diogo, 2020). A key challenge of this method is to maximize ore recovery and extraction efficiency while minimizing waste production. This method is generally considered cost-effective when the surrounding rock can be excavated safely and efficiently. It also tends to have a smaller environmental footprint than surface mining approaches (Ghorbani et al., 2023). The process involves developing shafts and production galleries, with excavation usually carried out by drilling and blasting. Once extracted, the ore is transported to the surface for processing and concentration (Osmanlioglu, 2022).

Underground uranium mining typically involves either wet or dry drilling methods accompanied by the use of electrical or diesel powered equipment (Marsh et al., 2008; ICRP, 2017). These methods have distinct operational procedures and health implications for miners, particularly with regard to exposure to radon gas and its progeny. The main differences between the two methods lie in the strategies used to suppress dust and the efficiency of ventilation systems in mitigating radiological and respiratory hazards.

For purposes of dose assessment, miners are usually categorized according to their exposure conditions and levels of physical exertion. According to Marsh et al. (2008), underground mining activities generally involve three levels of physical activity i.e. low, moderate and high, with each of these categories corresponds to specific breathing rates i.e. 1.0 m^3/h for low exertion, 1.2 m^3/h for moderate exertion, and 1.4 m^3/h for high exertion. A brief description of the relevant mining techniques for this study is given in the following subsections.

2.1. Wet drilling with good ventilation (Job 1)

In wet drilling, water is used to suppress dust during the drilling process. This significantly reduces the number of airborne particulates, including radioactive dust containing radon progeny. Operations using this method are supported by forced or mechanically assisted ventilation systems that supply fresh air at rates of between 1.5 and 4.5 m^3/s per worker (Widodo et al., 2023). Good ventilation disperses radon gas and lowers the concentration of long-lived radioactive dust. Mine workers' duties include operating drilling rigs, installing support systems and

transporting ore.

When appropriate control measures are in place, exposure to radon progeny typically remains below 0.5 working level months (WLM)[1] per year (Hoffman et al., 2007). Miners performing Job 1 are exposed to lower levels of radiation and are therefore less likely to develop occupational illnesses associated with uranium mining, such as pneumoconiosis and lung cancer.

2.2. Dry drilling with poor ventilation (Job 4)

Dry drilling omits water based dust suppression. This, when combined with poor ventilation, often at a rate between 0.1 and 0.6 m^3/s per worker (Li et al., 2019), creates hazardous working conditions. This environment allows radon gas and its short-lived progeny to accumulate in the mine, resulting in significantly higher exposure levels to the miners (Kreuzer et al., 2008).

Historically, exposure levels in dry drilling operations often exceeded 5–10 WLM/year (Samet and Hornung, 1990). Miners performing this job type must clear dust and debris more frequently and endure intense physical labor in confined, poorly ventilated areas. Under these mining conditions, the absence of effective airflow results in radon progeny being retained for longer in breathing zones, sharply increasing the risk of lung cancer (Grosche et al., 2006).

A study conducted by Lubin et al. (1995) directly links dry drilling in poorly ventilated conditions to an increased risk of radiogenic lung cancer, as evidenced by cohort studies of uranium miners in Canada and the United States of America.

3. Materials and methods

3.1. Biokinetic models

The ICRP latest biokinetic models were used in this study to calculate the committed equivalent dose coefficients. These models include, the Human Respiratory Tract Model (HRTM) published in ICRP publication 130 (ICRP, 2015), Human Alimentary Tract Model (HATM) published in ICRP publication 100 (ICRP, 2006) and the systemic models of polonium, lead and bismuth published in ICRP publication 137 (ICRP, 2017).

3.2. Implementation of the ICRP methodology for internal dose assessment in INTDOSKIT

The INTDOSKIT tool was designed such that all the information on the biokinetics and dosimetry is imported from plain text input files. This has the advantages of making it possible to handle any radionuclide without any modifications in the source code in addition to minimizing the size of the source program (Breustedt et al., 2024).

The tool comprises four main libraries, each of which is implemented as an R script and provides distinct functions within the dose assessment framework. The first library is the deposition model functions library, which calculates the deposition fractions of inhaled radioactive aerosols across various regions of the HRTM. The second library contains functions for defining and solving biokinetic models to determine the retention and excretion of radioactive substances in different compartments over time. It also calculates the number of radioactive decays within ICRP-defined source regions.

The third library contains dosimetric functions, which are responsible for computing S-coefficients, effective doses and organ-specific doses for both ICRP target tissues and radiosensitive tissues. Lastly, the constants library provides essential parameters such as ICRP radiation and tissue weighting factors, unit conversion factors, lists of source and target organs, and recommended time steps for generating retention and excretion curves.

These libraries are sourced at the beginning of the dose calculations such that the required functions can be called during program execution instead of hard coding them in the main program. Templates of R scripts for typical tasks were developed and guidance on their use is provided in the documentation of INTDOSKIT (Breustedt et al., 2024).

Fig. 1 shows the steps in the ICRP methodology for calculating dose coefficients as implemented in INTDOSKIT for this study. Reference dose coefficients were calculated using ICRP input data for a reference adult male and female and then validated against values obtained from the ICRP OIR Dataviewer software. The percentage deviation of the calculated values for both males and females was determined using equation (1). Further details on INTDOSKIT can be found in Breustedt et al. (2024).

$$Percentage\ deviation = \left(\frac{Calculated\ value - ICRP\ value}{ICRP\ value}\right) x100 \quad (1)$$

3.3. Assignment of probability distributions to model parameters

Probability distributions for the aerosol parameters in underground mines for the two exposure scenarios in this work as well as probability distributions for the HRTM model parameters for particle deposition and clearance were taken from Makumbi et al. (2024a). Additionally, probability distribution for the HATM model parameters were taken from Kwon et al. (2020).

Probability distributions for the absorption parameters of radon progeny were derived from several studies (Booker et al., 1969; Hursh et al., 1969; Hursh and Mercer, 1970; Boudene et al., 1977; Chamberlain et al., 1978; Greenhalgh et al., 1982; James et al., 1977; Butterweck et al., 2002; Marsh and Birchall, 2000; ICRP, 2017). These distributions account for variations in dissolution fractions, absorption and transfer rates of lead, bismuth and polonium.

For lead as radon progeny, the rapid dissolution fraction (f_r) varies from 0.06 (Booker et al., 1969) to 0.35(Greenhalgh et al., 1982), with other reported values ranging between 0.1 and 0.2 (James et al., 1977; Marsh and Bailey, 2013; ICRP, 2017). Based on these data, a uniform probability distribution with a minimum value of 0.06 and a maximum value of 0.12 was adopted.

The rapid dissolution rate (s_r) shows significant variation ranging from 58 d^{-1} (Greenhalgh et al., 1982) to 1000 d^{-1}(Butterweck et al., 2002), with additional reported values of 67 d^{-1}, 100 d^{-1} and 250 d^{-1}(ICRP, 2017). Due to this broad range, a lognormal distribution was assigned to this parameter, with a geometric mean (GM)[2] of 100 d^{-1} (ICRP reference value) and geometric standard deviation (GSD)[3] of 3.20.

In contrast, slow dissolution rates (s_s) are more consistent, ranging from 1.3 d^{-1} (Hursh et al., 1969) to 1.8 d^{-1} (James et al., 1977). Given the minimal variation, a uniform probability distribution with a minimum value of 1.3 d^{-1} and maximum value of 1.8 d^{-1} was adopted for this parameter. Similarly, the transfer rate of lead ions (s_b) to blood varies significantly, with reported values spanning from 0.5 d^{-1} (Boudene et al., 1977) to 5.7 d^{-1} (Chamberlain et al., 1978). For this

[1] The historical unit used to measure exposure to radon progeny in uranium mining is WLM; defined as the cumulative exposure from breathing an atmosphere at a concentration of one working level (WL) for a working month of 170 h. WL refers to any combination of short-lived radon progeny in 1 m^3 of air that results in the emission of 1.30E+08 MeV of alpha energy (ICRP, 1993, 2017).

[2] GM is a statistical parameter that indicates the aggregation or typical value of a group of quantitative observations by using a product of their values. It is a measure of central tendency for skewed data that follows a lognormal distribution and is calculated as the n^{th} root of the product of n numbers (Vogel, 2020; Mbaji et al., 2023).

[3] GSD is a statistical parameter that is used to quantify the spread or dispersion of data that is skewed or follows a lognormal distribution in relation to GM (Martinez and Bartholomew, 2017).

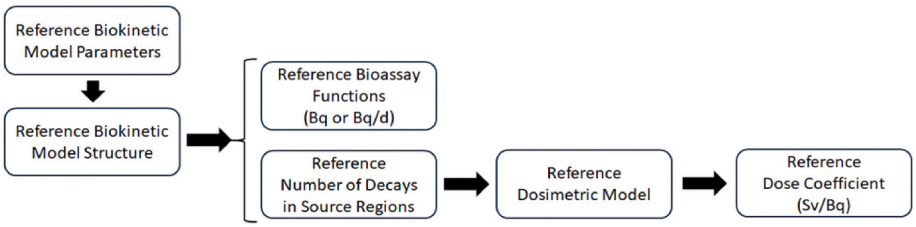

Fig. 1. Summary of the ICRP methodology for internal dose assessment that was implemented in INTDOSKIT.

parameter, a lognormal distribution was assigned with GM of 1.7 d^{-1} (ICRP reference value) and a GSD of 1.73.

Literature studies showed a variation in the proportion of lead bound to the respiratory epithelium. A study conducted by Moody et al. (1994) reported a value of 0.25, whereas Butterweck et al. (2002) estimated a range between 0.70 and 0.85. Other reported values include 0.32 (Greenhalgh et al., 1982), 0.40 (Booker et al., 1969), 0.50 (ICRP, 2017) and 0.70 (Marsh and Bailey, 2013). Based on these data, the authors modelled this parameter using a uniform probability distribution with bounds from 0.25 to 0.70.

For isotopes of polonium and bismuth as radon progeny, the latest ICRP publications provide distinct absorption parameters for these elements, assuming no epithelial binding and classifying them under type F absorption (ICRP, 2017; Makumbi et al., 2024a). As a result, f_r for both bismuth and polonium were assigned a uniform probability distribution with a minimum value of 0.70 and a maximum value of 1.00. Additionally, s_r for each of these two progenies was assigned a lognormal distribution using the ICRP reference value as GM and a GSD of 3.20. Probability distributions for the absorption parameters of short-lived radon progeny used in this work are presented in Table 1.

Table 1
Probability distributions for dissolution/absorption parameters for radon progeny.

Nuclide	Parameter	Reference value[a]	Probability distribution	A[b]	B[c]
Polonium	f_r	1.00	uniform	0.70	1.00
	s_r	3.00	lognormal	3.00	3.20
	s_s	0.00	constant		
	f_b	0.00	constant		
	s_b	0.00	constant		
	f_A	0.10	$0.10*f_r$[d]		
Lead	f_r	0.10	uniform	0.06	0.12
	s_r	100.00	lognormal	100.00	3.20
	s_s	1.70	uniform	1.30	1.80
	f_b	0.50	uniform	0.25	0.70
	s_b	1.70	lognormal	1.70	1.73
	f_A	0.20	$0.20*f_r$[d]		
Bismuth	f_r	1.00	uniform	0.70	1.00
	s_r	1.00	lognormal	1.00	3.20
	s_s	0.00	constant		
	f_b	0.00	constant		
	s_b	0.00	constant		
	f_A	0.05	$0.05*f_r$[d]		

f_r: Rapid dissolution fraction; s_r: Rapid dissolution rate (d^{-1}); s_s: Slow dissolution rate (d^{-1}); f_b: Bound fraction; s_b: Dissolution rate for the bound fraction material (d^{-1}); f_A: Fraction of material absorbed from the HATM to blood.

[a] Data taken from ICRP, 2017.

[b] Minimum value for a uniform distribution or GM for a lognormal distribution.

[c] Maximum value for a uniform distribution or GSD for a lognormal distribution.

[d] The probability distribution for f_A parameter is derived from a correlation with f_r i.e., uncertainty is introduced on this parameter by multiplying the ICRP reference value for ingestion of the element with the sampled value of the f_r parameter from its respective probability distribution during Monte Carlo simulation.

3.4. Monte Carlo methods for uncertainty and sensitivity analysis

To assess the uncertainties in the dose coefficients from inhalation of radon progeny, a parameter uncertainty analysis was performed using Monte Carlo simulations. In this approach, probability distributions were assigned to the model parameters, taking into account correlations between them. These uncertainties were then incorporated directly into the dose calculation methodology.

The extended version of INTDOSKIT, an in-house software tool developed by the authors for uncertainty and sensitivity analysis of calculated doses, was used to accomplish this task. The Monte Carlo method used in this study was the same as that described in an earlier study by the authors (Makumbi et al., 2024b). This method is graphically presented in Fig. 2.

To perform a sensitivity analysis on the calculated dose coefficients, the model parameters of interest were grouped into particle deposition parameters, absorption parameters and particle transport parameters. The particle deposition parameters were themselves grouped into three (3) sub categories and these included activity parameters such as tidal volume (V_T), breathing frequency (f_R), breathing rate (B), fraction of air breathed through the nose (F_n) and the fraction of time spent in each activity by the subject; aerosol parameters such as particle size (AMAD/AMTD) and dispersion (σ), particle density (ρ), shape factor (χ) and hygroscopic growth factor (hgf); subject parameters such as dead space volume (V_D) and functional residual capacity (FRC).

The methodology for the sensitivity of dose coefficients to uncertainty in the particle deposition model parameters, absorption parameters for radon progeny and particle transport parameters is captured in Table 2. To achieve this, the model parameters of interest were varied by randomly sampling each parameter from its corresponding probability distribution, while keeping all other parameters fixed at their respective ICRP reference values.

As an illustration, to assess the impact of absorption parameters on the committed equivalent lung dose coefficient, these parameters were sampled from their respective probability distributions (see Table 1) in each Monte Carlo simulation run, while all other parameter groups such as activity, subject, aerosol, and particle transport were held constant at their respective ICRP reference values. This approach corresponds to calculation method (i) in Table 2. In a separate simulation, the absorption parameters were fixed at their ICRP reference values, while the other parameter groups were varied by sampling from their respective distributions in each run. This corresponds to calculation method (ii) in Table 2. Calculation approach (ii) was necessary to assess the relative influence of the absorption parameters with reference to the other parameter groups. The above procedure was repeated to enable a comparison of the influence of each parameter or group of parameters as outlined in Table 2.

3.5. Fitting a probability distribution to the generated posterior data set

A probability distribution was fitted to the posterior data set in INTDOSKIT using maximum likelihood estimation (MLE) and the Kolmogorov-Smirnov (K-S) test using functions of the fitdistrplus library of R (Makumbi et al., 2024b).

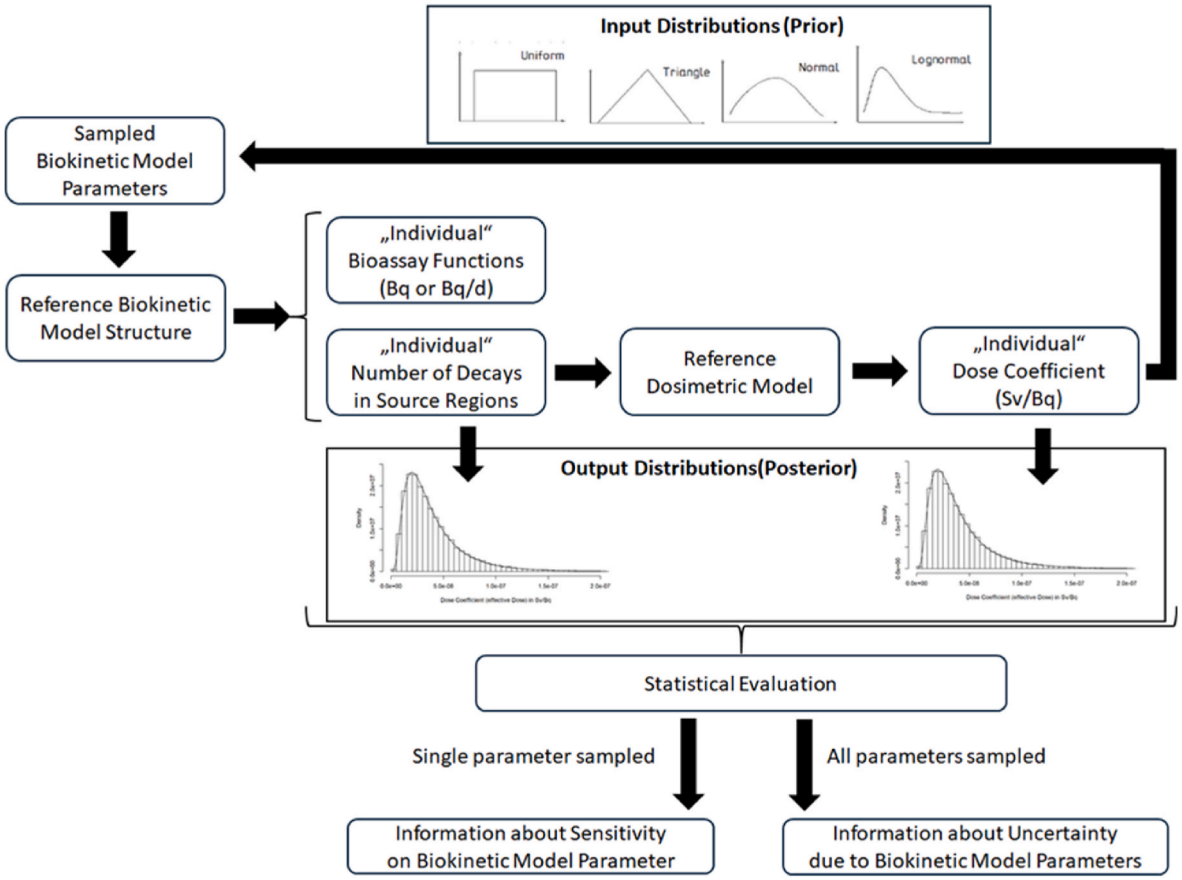

Fig. 2. Monte Carlo method for uncertainty and sensitivity studies used in this work (Source: Makumbi et al., 2024b).

Table 2
Monte Carlo simulation method for sensitivity analysis used in this work.

Parameters for sensitivity analysis focus	Monte Carlo simulation modifications
Activity	i) Vary activity parameters; fix all others at ICRP reference values ii) Fix activity parameters at ICRP reference values; vary all others.
Aerosol	i) Vary aerosol parameters; fix all others at ICRP reference values. ii) Fix aerosol parameters at ICRP reference values; vary all others.
Subject	i) Vary subject parameters; fix all others at ICRP reference values. ii) Fix subject parameters at ICRP reference values; vary all others.
Absorption	i) Vary absorption parameters; fix all others at ICRP reference values. ii) Fix absorption parameters at ICRP reference values; vary all others.
Particle transport	i) Vary particle transport parameters; fix all others at ICRP reference values. ii) Fix particle transport parameters at ICRP reference values; vary all others.

3.6. Comparison of the two job types using a hypothesis test

To determine whether simulation outputs from the two exposure scenarios were statistically distinct, non-parametric hypothesis tests were applied. Specifically, the Mann–Whitney *U* test (implemented via wilcox.test function in base R) was used to detect differences in central tendency without making a normality assumption.

4. Results and Discussions

4.1. Validation of INTDOSKIT calculations against ICRP data

Table 3 shows the results of the committed equivalent dose coefficient calculations performed by INTDOSKIT using the ICRP reference data. It also shows the validation using the ICRP data. The findings demonstrate that INTDOSKIT reliably models radon progeny decay chains. Specifically, the dose coefficients calculated for the inhalation of radon progeny in underground mining environments are in good agreement with the ICRP reference values; the largest observed deviation is ±6 %.

4.2. Dose calculations for the inhalation of radon progeny in underground mines

The results of the committed equivalent dose coefficients calculated are presented in Table 4 for the two exposure scenarios. The calculated equivalent organ and tissue dose coefficients (mSv/(mJh/m^3)) for these scenarios show variations in radiation exposure at different anatomical sites due to the inhalation of radon progeny in underground mines.

From Table 4 and it can be observed that the highest dose coefficients are associated to the respiratory tract, particularly in the central airways, where radon progeny particles are likely to deposit due to their particle size and inhalation characteristics. Specifically, Bronch.sec and Bronch.bas received the highest doses, with Job 4 showing significantly higher values (8.67E+01 mSv/(mJh/m^3) for Bronch.sec and 4.22E+01 mSv/(mJh/m^3) for Bronch.bas) compared to Job 1 (4.61E+01 mSv/(mJh/m^3) and 2.10E+01 mSv/(mJh/m^3), for Bronch.sec and Bronch.bas respectively). This implies a greater risk of radiation-induced damage in these regions for workers performing Job 4.

Table 3
Committed dose coefficients (mSv/(mJh/m^3)[41]) due to inhalation of radon progeny in underground mines calculated using ICRP reference data.

Organ/Tissue	INTDOSKIT (mSv/(mJh/m^3))		ICRP (mSv/(mJh/m^3))		Male Deviation (%)	Female Deviation (%)
	Male	Female	Male	Female		
Bone marrow	4.5E-03	5.6E-03	4.3E-03	5.4E-03	5	4
Colon	4.2E-03	4.7E-03	4.0E-03	4.5E-03	5	4
Lung	2.5E+01	2.6E+01	2.4E+01	2.6E+01	4	0
Stomach	7.2E-03	7.8E-03	6.9E-03	7.6E-03	4	3
Breast	2.3E-03	2.7E-03	2.2E-03	2.6E-03	5	4
Gonads	1.7E-03	3.5E-03	1.8E-03	3.6E-03	−6	−3
Urinary bladder	1.9E-03	2.3E-03	1.9E-03	2.3E-03	0	0
Oesophagus	6.1E-03	7.4E-03	5.8E-03	7.1E-03	5	4
Liver	1.3E-02	1.7E-02	1.3E-02	1.7E-02	0	0
Thyroid	3.4E-03	4.3E-03	3.3E-03	4.1E-03	3	5
Bone surface	1.2E-02	1.4E-02	1.2E-02	1.4E-02	0	0
Brain	2.1E-03	2.4E-03	2.0E-03	2.4E-03	5	0
Salivary glands	2.1E-03	2.5E-03	2.1E-03	2.5E-03	0	0
Skin	1.4E-03	1.9E-03	1.4E-03	1.9E-03	0	0
Adrenals	3.8E-03	4.4E-03	3.7E-03	4.2E-03	3	5
Gall bladder	2.2E-03	2.5E-03	2.2E-03	2.4E-03	0	4
Heart	4.2E-03	5.6E-03	4.0E-03	5.4E-03	5	4
Kidneys	5.3E-02	6.2E-02	5.4E-02	6.4E-02	−2	−3
Muscle	1.9E-03	2.2E-03	1.8E-03	2.2E-03	6	0
Oral mucosa	2.8E-03	3.5E-03	2.7E-03	3.4E-03	4	3
Pancreas	3.8E-03	4.5E-03	3.7E-03	4.4E-03	3	2
Prostate	1.9E-03	0	1.9E-03	0	0	0
Small intestine	4.4E-03	5.1E-03	4.3E-03	5.0E-03	2	2
Spleen	5.2E-03	6.3E-03	5.1E-03	6.2E-03	2	2
Thymus	2.9E-03	3.5E-03	2.8E-03	3.4E-03	4	3
Uterus	0	2.2E-03	0	2.2E-03	0	0
e (50)[a]	3.17		3.14		1	

[a] e (50) refers to the committed effective dose coefficient.

Table 4
Calculated equivalent organ and tissue dose coefficients (mSv/(mJh/m^3)) from inhalation of radon progeny in underground mines for the two exposure scenarios.

Organ/Tissue	Job 1	Job 4
Lung	1.50E+01	2.33E+01
Bronch.bas	2.10E+01	4.22E+01
Bronch.sec	4.61E+01	8.67E+01
Bchiol.sec	2.90E+01	4.71E+01
AI	1.72E+00	2.44E+00
St. stem	1.30E-02	2.60E-02
R.marrow	4.45E-03	7.28E-03
Colon	1.97E-03	2.87E-03
RC.stem	4.37E-03	7.25E-03
LC.stem	4.42E-03	7.37E-03
RS.stem	3.94E-03	6.38E-03
Liver	5.73E-03	8.24E-03
Kidneys	5.12E-02	8.27E-02
Endost.BS	1.15E-02	1.88E-02
Brain	1.09E-03	1.70E-03
Ht.wall	4.09E-03	6.70E-03

Bronch.bas: Bronchial basal cells; Bronch.sec: Bronchial secretory cells; Bchiol.sec: Bronchiolar secretory cells; AI: Alveolar-interstitial; St.stem: stomach stem cells; R.marrow: Red-marrow; RC.stem: Right colon stem cells; LC.stem: Left colon stem cells; RS.stem: Rectosigmoid colon stem cells; Endost.BS: Endosteal bone surface; Ht.wall: Heart wall.

The high dose value of Bronch.sec is due to its relatively small tissue mass and close proximity to the deposition sites of alpha-emitting radon progeny, which results in elevated SAF values. It can be argued that although the Bronch.bas region has a smaller tissue mass, its greater distance from the source regions reduces its dose. In contrast, the AI region receives the lowest dose due to its large mass (1.1 kg) and reduced particle deposition in deeper lung regions, which leads to lower SAF values.

The lung tissue itself also received significant doses, with values of 1.50E+01 mSv/(mJh/m^3) for Job 1 and 2.33E+01 mSv/(mJh/m^3) for Job 4, reinforcing the importance of lung exposure in the assessment of radon-related radiation risk. Beyond the respiratory tract, the systemic distribution of radon progeny results in lower but non-negligible dose coefficients in other organs. The kidneys and Endost.BS show relatively higher dose coefficients compared to other systemic organs and tissues, with kidney doses increasing from 5.12E-02 mSv/(mJh/m^3) (Job 1) to 8.27E-02 mSv/(mJh/m^3) (Job 4). This may be attributed to the biokinetics of short-lived radon progeny, particularly the alpha-emitting polonium isotopes i.e. following inhalation or exposure through a wound, polonium is typically rapidly excreted in urine a pattern that is absent or significantly less pronounced after exposure through other routes (Leggett and Eckerman, 2001; ICRP, 2017).

The target regions St.stem, R.marrow, colon and liver received relatively low doses, remaining in the range of 10^{-2} to 10^{-3} mSv/(mJh/m^3), indicating a significantly lower contribution of radon progeny to the radiation burden in these tissues. The brain and Ht.wall target regions also showed minimal exposure, with dose coefficients below 7.00E-03 mSv/(mJh/m^3), suggesting a lesser effect of radon progeny on these tissues.

Across all organs and tissues, Job 4 had consistently higher dose coefficients than Job 1. This confirms that the exposure conditions in Job 4 lead to greater inhalation of radon progeny, due to factors such as higher airborne radon concentrations and differences in workplace ventilation. The most pronounced increase was observed in the central airways, where dose coefficients were almost doubled in Job 4 compared to Job 1, highlighting the increased risk of lung cancer and other respiratory diseases in higher exposure scenarios.

The significantly higher doses in Job 4 suggest the need for improved ventilation, exposure monitoring and protective measures in high-risk underground mining environments. The systemic radiation doses, although lower, reinforce the need for comprehensive dosimetric evaluations to assess long-term health effects in underground miners.

4.3. Uncertainty on committed equivalent dose coefficients from inhalation of radon progeny in underground mines

During the Monte Carlo simulations, the convergence of the final

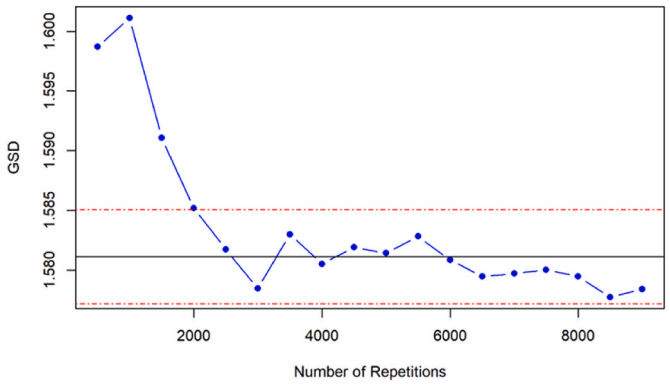

Fig. 3. Test for convergence of the dataset. The x-axis gives the number of repetitions and the y-axis shows the GSD of the distribution of the committed equivalent lung dose coefficient. The solid line gives the final GSD of the whole dataset of 50,000 repetitions, dash dotted lines indicate ±0.2 % range around this value.

dataset with 50,000 repetitions (obtained from the central limit theorem) was tested by recalculating the GSD of the distribution of the committed equivalent lung dose coefficient after every 500th run. Fig. 3 shows the GSD of this distribution against the number of iterations. From Fig. 3, the values of the first 2,000 runs show a larger fluctuation with GSD values ranging from 1.585 to 1.630. After 2,500 runs, the fluctuations are within ±0.2 % of the GSD of the whole dataset of 1.58. Therefore, it was confirmed that 50,000 runs ensured the desired convergence.

A global uncertainty analysis was conducted to evaluate uncertainties of the committed equivalent lung dose coefficients resulting from the inhalation of radon progeny in underground mining scenarios. The results, are presented in Tables 5 and 6 for Job1 and Job 4 respectively. For Job 1, the GM dose coefficient is 47.05 mSv/(mJh/m^3), with GSD of 1.58. The 95 % confidence interval (CI) ranges from 18.59 to 104.74 mSv/(mJh/m^3) and the uncertainty factor (UF)[5] is 2.37. For Job 4, the GM increases to 61.87 mSv/(mJh/m^3) (GSD = 1.56), with a CI ranging from 24.83 to 133.09 mSv/(mJh/m^3) and UF of 2.32.

Right-skewed distributions are evident in both scenarios, as indicated by mean values slightly exceeding their corresponding medians. This reflects the influence of extreme values, which are typical of skewed distributions such as the lognormal distribution for most model parameters used in the Monte Carlo simulations.

The highest uncertainty occurs in the AI region (UF = 3.32 for Job 1 and 3.13 for Job 4), while the lowest lung dose uncertainty occurs in the Bchiol.sec and Bronch.bas regions for Job 1 (UF = 2.49) and in the Bchiol.sec region for Job 4 (UF = 2.29). Outside of the lung, the kidneys exhibit the greatest uncertainty (UF = 2.88 for Job 1 and 2.75 for Job 4) while the St.stem region is associated with the lowest systemic uncertainty (UF = 2.53 for Job 1 and 2.32 for Job 4).

In Job 1, the mean dose coefficient of 52.01 mSv/(mJh/m^3) is 2.2 times higher than the ICRP reference value of 24.00 mSv/(mJh/m^3) given in Table 3, while the median is 48.48 mSv/(mJh/m^3), which is higher than the ICRP reference value by a factor of 2. The 97.5th percentile (Q_U) of 104.74 mSv/(mJh/m^3) indicates considerable variation in higher dose outcomes, while the 2.5th percentile (Q_L) of 18.59 mSv/(mJh/m^3) suggests more limited uncertainty in the lower range. In Job 4, the mean rises to 67.98 mSv/(mJh/m^3) (2.8 times the ICRP value) and the median to 63.73 mSv/(mJh/m^3) (2.7 times higher). Meanwhile, Q_U extends to 133.09 mSv/(mJh/m^3), highlighting greater uncertainty at the upper end, although the Q_L value of 24.83 mSv/(mJh/m^3) closely

[5] UF here is defined as the square root of the quotient of the 97.5th percentile to the 2.5th percentile value.

Table 5
Summary statistics for organ and tissue dose coefficients (mSv/(mJh/m^3)) from inhalation of radon progeny by underground miners under Job 1 exposure conditions.

Organ	Undisturbed	Mean	SD	GM	GSD	UF	Min	X2.5	X5.0	X25	X50	X75	X95	X97.5	Max
Lung	1.50E + 01	5.20E + 01	2.30E + 01	4.70E+01	1.58E+00	2.37E+00	8.70E+00	1.86E+01	2.12E+01	3.41E+01	4.84E+01	6.62E+02	9.52E+01	1.05E+02	1.67E+02
Bronch.bas	2.10E + 01	4.58E + 01	2.17E + 01	4.10E+01	1.61E+00	2.49E+00	5.92E+00	1.57E+01	1.81E+01	2.94E+01	4.18E+01	5.80E+01	8.66E+01	9.80E+01	1.94E+02
Bronch.sec	4.61E + 01	1.12E + 02	5.32E + 01	1.00E+02	1.61E+00	2.49E+00	1.45E+01	3.85E+01	4.42E+01	7.20E+01	1.02E+02	1.42E+02	2.12E+02	2.40E+02	4.77E+02
Bchiol.sec	2.90E + 01	7.28E + 01	3.43E + 01	6.51E+01	1.62E+00	2.51E+00	1.28E+01	2.44E+01	2.83E+01	4.65E+01	6.69E+01	9.29E+01	1.37E+02	1.54E+02	2.69E+02
AI	1.72E + 00	4.34E + 00	2.56E + 00	3.57E+00	1.93E+00	3.32E+00	4.96E-01	9.24E-01	1.09E+00	2.22E+00	3.91E+00	5.99E+00	9.16E+00	1.02E+01	1.69E+01
St.stem	1.30E - 02	2.17E - 02	1.02E - 02	1.93E-02	1.63E+00	2.53E+00	2.84E-03	7.08E-03	8.20E-03	1.38E-02	2.01E-02	2.79E-02	4.09E-02	4.52E-02	7.38E-02
R.marrow	4.45E - 03	8.93E - 03	4.69E - 03	7.70E-03	1.76E+00	2.84E+00	1.17E-03	2.45E-03	2.83E-03	5.10E-03	8.19E-03	1.19E-02	1.78E-02	1.97E-02	3.08E-02
Colon	1.97E - 03	8.87E - 03	4.62E - 03	7.67E-03	1.75E+00	2.80E+00	1.16E-03	2.47E-03	2.86E-03	5.10E-03	8.13E-03	1.18E-02	1.76E-02	1.94E-02	3.01E-02
RC.stem	4.37E - 03	8.98E - 03	4.66E-03	7.77E-03	1.75E+00	2.79E+00	1.18E-03	2.52E-03	2.91E-03	5.18E-03	8.23E-03	1.20E-02	1.78E-02	1.96E-02	3.03E-02
LC.stem	4.42E - 03	9.05E - 03	4.69E-03	7.83E-03	1.75E+00	2.79E+00	1.19E-03	2.54E-03	2.94E-03	5.22E-03	8.30E-03	1.21E-02	1.79E-02	1.98E-02	3.05E-02
RS.stem	3.94E - 03	8.29E - 03	4.38E-03	7.13E-03	1.77E+00	2.86E+00	1.06E-03	2.25E-03	2.60E-03	4.71E-03	7.58E-03	1.11E-02	1.66E-02	1.83E-02	2.91E-02
Liver	5.73E - 03	2.60E - 02	1.38E-02	2.24E-02	1.77E+00	2.86E+00	3.37E-03	7.04E-03	8.15E-03	1.48E-02	2.38E-02	3.48E-02	5.20E-02	5.75E-02	9.11E-02
Kidneys	5.12E - 02	1.05E - 01	5.57E-02	8.99E-02	1.78E+00	2.88E+00	1.36E-02	2.80E-02	3.26E-02	5.92E-02	9.56E-02	1.40E-01	2.10E-01	2.32E-01	3.70E-01
Endost.BS	1.15E - 02	2.18E - 02	1.15E-02	1.88E-02	1.76E+00	2.84E+00	2.89E-03	5.96E-03	6.90E-03	1.24E-02	2.00E-02	2.91E-02	4.34E-02	4.79E-02	7.47E-02
Brain	1.09E - 03	4.43E - 03	2.27E-03	3.85E-03	1.73E+00	2.75E+00	6.09E-04	1.27E-03	1.46E-03	2.58E-03	4.08E-03	5.89E-03	8.73E-03	9.61E-03	1.44E-02
Ht.wall	4.09E - 03	8.35E - 03	4.38E-03	7.20E-03	1.76E+00	2.83E+00	1.11E-03	2.29E-03	2.64E-03	4.77E-03	7.66E-03	1.12E-02	1.66E-02	1.83E-02	2.88E-02

SD: Standard deviation; GM: Geometric mean; GSD: Geometric standard deviation; UF: uncertainty factor; Min: minimum value; X2.5: 2.5th percentile; X5.0: 5th percentile; X25: 25th percentile; X50: 50th percentile; X75: 75th percentile; X95: 95th percentile; X97.5: 97.5th percentile; Max: Maximum value; Undisturbed: Reference dose value for the exposure scenario.

Table 6
Summary statistics for organ and tissue dose coefficients (mSv/(mJh/m^3)) from inhalation of radon progeny by underground miners under Job 4 exposure conditions.

Organ	Undisturbed	Mean	SD	GM	GSD	UF	Min	X2.5	X5.0	X25	X50	X75	X95	X97.5	Max
Lung	2.33E+01	6.80E+01	2.90E+01	6.19E+01	1.56E+00	2.32E+00	1.48E+01	2.48E+01	2.84E+01	4.53E+01	6.37E+01	8.64E+01	1.22E+02	1.33E+02	1.99E+02
Bronch.bas	4.22E+01	6.18E+01	2.72E+01	5.61E+01	1.57E+00	2.36E+00	1.24E+01	2.25E+01	2.57E+01	4.10E+01	5.74E+01	7.81E+01	1.13E+02	1.25E+02	1.99E+02
Bronch.sec	8.67E+01	1.49E+02	6.56E+01	1.35E+02	1.57E+00	2.36E+00	2.99E+01	5.42E+01	6.20E+01	9.91E+01	1.39E+02	1.89E+02	2.73E+02	3.02E+02	4.77E+02
Bchiol.sec	4.71E+01	9.32E+01	3.90E+01	8.51E+01	1.55E+00	2.29E+00	2.12E+01	3.42E+01	3.92E+01	6.24E+01	8.79E+01	1.19E+02	1.66E+02	1.79E+02	2.53E+02
AI	2.44E+00	5.12E+00	2.86E+00	4.29E+00	1.87E+00	3.13E+00	6.57E-01	1.17E+00	1.38E+00	2.74E+00	4.69E+00	7.02E+00	1.05E+01	1.15E+01	1.64E+01
St.stem	2.60E-02	2.79E-02	1.19E-02	2.53E-02	1.57E+00	2.32E+00	6.25E-03	1.01E-02	1.15E-02	1.84E-02	2.62E-02	3.56E-02	5.00E-02	5.43E-02	7.32E-02
R.marrow	7.28E-03	1.09E-02	5.43E-03	9.47E-03	1.72E+00	2.72E+00	1.78E-03	3.12E-03	3.63E-03	6.41E-03	1.01E-02	1.44E-02	2.10E-02	2.30E-02	3.24E-02
Colon	2.87E-03	1.08E-02	5.36E-03	9.45E-03	1.71E+00	2.69E+00	1.81E-03	3.15E-03	3.66E-03	6.42E-03	1.00E-02	1.43E-02	2.08E-02	2.28E-02	3.22E-02
RC.stem	7.25E-03	1.09E-02	5.41E-03	9.58E-03	1.70E+00	2.68E+00	1.85E-03	3.21E-03	3.73E-03	6.52E-03	1.02E-02	1.45E-02	2.11E-02	2.30E-02	3.25E-02
LC.stem	7.37E-03	1.10E-02	5.46E-03	9.67E-03	1.70E+00	2.68E+00	1.86E-03	3.24E-03	3.77E-03	6.59E-03	1.03E-02	1.46E-02	2.12E-02	2.32E-02	3.27E-02
RS.stem	6.38E-03	1.00E-02	5.06E-03	8.75E-03	1.72E+00	2.74E+00	1.61E-03	2.85E-03	3.33E-03	5.91E-03	9.30E-03	1.34E-02	1.95E-02	2.14E-02	3.08E-02
Liver	8.24E-03	3.15E-02	1.59E-02	2.75E-02	1.73E+00	2.74E+00	5.07E-03	8.95E-03	1.04E-02	1.85E-02	2.92E-02	4.20E-02	6.13E-02	6.70E-02	9.59E-02
Kidneys	8.27E-02	1.27E-01	6.43E-02	1.10E-01	1.72E+00	2.75E+00	2.01E-02	3.58E-02	4.16E-02	7.43E-02	1.18E-01	1.69E-01	2.47E-01	2.71E-01	3.88E-01
Endost.BS	1.88E-02	2.65E-02	1.33E-02	2.31E-02	1.73E+00	2.72E+00	4.34E-03	7.59E-03	8.84E-03	1.56E-02	2.46E-02	3.52E-02	5.13E-02	5.61E-02	7.82E-02
Brain	1.70E-03	5.44E-03	2.66E-03	4.79E-03	1.72E+00	2.64E+00	9.49E-04	1.63E-03	1.89E-03	3.28E-03	5.06E-03	7.19E-03	1.04E-02	1.14E-02	1.58E-02
Ht.wall	6.70E-03	1.02E-02	5.08E-03	8.88E-03	1.69E+00	2.71E+00	1.71E-03	2.92E-03	3.40E-03	6.02E-03	9.43E-03	1.35E-02	1.97E-02	2.15E-02	3.02E-02

SD: Standard deviation; GM: Geometric mean; GSD: Geometric standard deviation; UF: uncertainty factor; Min: minimum value; X2.5: 2.5th percentile; X5.0: 5th percentile; X25: 25th percentile; X50: 50th percentile; X75: 75th percentile; X95: 95th percentile; X97.5: 97.5th percentile; Max: Maximum value; Undisturbed: Reference dose value for the exposure scenario.

approximates the ICRP benchmark.

The significant deviation of the medians from the ICRP reference values for the two job types can be attributed to the non-linear relationship between dose coefficients and model parameters. This is because the mean or median values of the parameter probability distributions used in the Monte Carlo simulations were not always the same as the ICRP reference values for these parameters. Another possible factor is the choice of probability distributions. While the selection of probability distributions was demonstrated to have a relatively minor effect on the central values and ranges of calculated dose distributions when constant variance in parameter uncertainties was assumed (Klein et al., 2010; Puncher and Harrison, 2012), this was not applicable to this study. The discrepancy between the median dose values obtained and the ICRP reference values can therefore be explained.

The wide uncertainty range (Q_L to Q_U), which is about an order of magnitude, reflects significant variation in the calculated dose coefficients due to uncertainties in the model parameters. For conservative safety assessments, it may therefore be prudent to consider values higher than the ICRP reference. While the ICRP reference value can still be used as a protective measure, incorporating additional statistical measures and considering distributional characteristics could enhance protection. This can be achieved by making adjustments to the reference value based on higher percentiles (e.g. the 75th or 95th), adopting the mean as the reference value, or revising biokinetic model parameters/biokinetic model structure to reduce the degree of skewness (Makumbi et al., 2024b).

These results underline the importance of considering both dose distribution and uncertainty when assessing the health risks associated with radon progeny inhalation. The variation in dose coefficients highlight the complexity of modelling dose distributions in the respiratory and systemic organs, particularly in high-risk occupational environments such as underground mines.

4.3.1. Comparison of committed equivalent dose coefficients from the two exposure scenarios

The comparison of the committed equivalent dose coefficients data between Job 1 and Job 4 as noted in Tables 5 and 6 show notable differences in dose metrics, reflecting both job type and lung region variation. This data shows that across all lung regions, Job 4 workers consistently receive higher doses than Job 1 workers; for instance, looking at the data for the lung and its target regions, the GM lung dose for Job 4 is 61.87 mSv/(mJh/m^3), compared with 47.05 mSv/(mJh/m^3) for Job 1. Similarly, in the Bronch.sec, the GM for Job 4 is 135.47 mSv/(mJh/m^3), significantly higher than 100.26 mSv/(mJh/m^3) for Job 1.

These differences are also reflected in the median and mean values, indicating that workers in Job 4 are at greater risk of higher doses in all lung regions, particularly in the Bchiol.sec and AI regions, where alpha radiation from radon progeny has limited penetration. However, the GSDs and UFs are comparable between the two job types, indicating similar variation in dose distribution within each lung region. The AI region shows the greatest uncertainty for both job types, with UFs of 3.32 for Job 1 and 3.13 for Job 4. This suggests considerable uncertainty in dose estimates for the deeper lung regions where deposition is more diffuse.

Statistically, the differences in dose between Job 1 and Job 4 could be significant, as indicated by Q_U. For example, the Q_U for the lung in Job 4 is 133.09 mSv/(mJh/m^3) compared to 104.74 mSv/(mJh/m^3) for Job 1, and for the Bronch.sec, Q_U is 302.34 mSv/(mJh/m^3) for Job 4 compared to 239.55 mSv/(mJh/m^3) for Job 1. The differences in dose values are also consistent in other organs and tissues outside the respiratory tract.

The differences in dose coefficients between job types suggest that workers in Job 4 environments are exposed to significantly higher levels of radon progeny, which has important health implications. From a radiological health perspective, the elevated doses received by Job 4 workers, particularly in the central airways, are concerning due to the

well-established link between exposure to radon progeny and an increased risk of lung cancer.

The combination of higher doses and greater uncertainty in Job 4 suggests that miners in this role are at an increased risk of radiation-induced health issues. These findings highlight the urgent need for targeted mitigation strategies in high-exposure work environments to minimize potential health risks.

Fig. 4 presents the graphical comparison of the results from the Monte Carlo simulation for the two exposure scenarios in form of grouped boxplots.

4.3.2. Statistical comparison of the two job types by hypothesis testing

The primary objective of hypothesis testing was to assess whether there were significant differences in organ-specific radiation dose coefficients between the two underground mining job types. The null hypothesis (H_0) was that the dose distributions (or their medians, assuming similarly shaped distributions) were similar in both job scenarios and the alternative hypothesis (H_1) was that the dose distributions for the two groups were not similar in both job scenarios.

However, because Monte Carlo simulations revealed that the dose data were positively skewed and could best be described by lognormal or gamma distributions, parametric methods such as the Welch *t*-test were deemed inappropriate (West, 2021). Hence, the Mann–Whitney *U* test was employed, as it is robust when comparing independent, non-normally distributed samples. Secondly, this distribution-free test compares the ranks of values between groups and is particularly well-suited to skewed datasets, which are common in radiation dose modelling (Nachar, 2008; Schober and Vetter, 2020; Tai et al., 2022).

This study involved 50,000 dose samples in each group (Job 1 and Job 4), resulting in an expected U-statistic[6] under the null hypothesis of 1.25E+09; calculated as the mean of the product of the number of iterations in the Monte Carlo simulations for the two job types. The value of 1.25E+09 represents the midpoint of the U distribution under the null hypothesis, assuming that the two groups have the same underlying distribution. Therefore, deviations from this value indicate differences in distributions.

From the data presented in Table 7, the observed U-statistics were much lower than 1.25 billion across all organs (e.g., 844,108,874 for the lungs) and the p-values were all 0 ($p < 1.0E\text{-}16$). Since the p-values are less than the limiting value of 0.05 for all organ and tissues, there was overwhelming evidence to reject the null hypothesis. The confidence intervals for the differences in medians were all negative, confirming the earlier notion of higher dose coefficients in Job 4 compared to Job 1. The largest differences were observed in the respiratory tract, particularly in Bronch.sec, with a median difference of up to −38 mSv/(mJh/m^3). Even systemic organs such as the kidneys, liver and brain showed significant dose increases, albeit to a lesser extent.

These results clearly confirm that Job 4 poses significantly higher radiation exposure risks than Job 1. The statistical evidence decisively supports the conclusion that the two job types are not equivalent in terms of exposure levels. These findings are also presented in form of a forest plot in Fig. 5.

4.3.3. Fitting probability distributions to the posterior datasets for the two job types

Figs. 6 and 7 show histograms of the committed equivalent lung dose coefficient (mSv/(mJh/m^3)) from radon progeny inhalation in underground mines under Job 1 and Job 4 exposure conditions, respectively. Both histograms show right-skewed distributions, indicating that most of the dose coefficients are concentrated at lower values, with a gradual decrease towards higher values. Superimposed on the histograms are fitted posterior distributions for the normal (blue), lognormal (red) and gamma (purple), providing insight into the best probabilistic representation of the data.

In both cases, the normal distribution fails to capture the right-skewed nature of the data as it assumes symmetry and does not adequately represent the long tail of higher dose coefficients. The lognormal distribution consistently provides the best fit, closely following the empirical data, particularly in capturing the peak and right tail behavior. The gamma distribution also performs well, although it deviates slightly in some regions. The preference for the lognormal and gamma distributions suggests that the lung dose coefficients result from multiplicative effects of independent factors such as variations in radon progeny concentration, breathing rates and particle deposition in the respiratory tract.

To validate the appropriateness of the fitted distribution, the Kolmogorov-Smirnov (K-S) test was employed as a goodness-of-fit measure. The K-S test was selected due to its non-parametric nature, sensitivity to differences between empirical and theoretical distributions, and its applicability across various sample sizes. Its straightforward interpretation and ability to uniformly assess test statistics further support its suitability for this analysis. Moreover, the K-S test offers the flexibility to evaluate multiple types of distributions, making it a robust choice for assessing the fit of complex models (Aslam, 2019; Lanzante, 2021; Cardoso and Galeno, 2023).

In contrast, other commonly used tests such as the Chi-square goodness-of-fit, Anderson-Darling, and Shapiro-Wilk tests were deemed less appropriate for this study because these methods exhibit limitations such as reduced effectiveness with small sample sizes, an inherent focus on normality, and inefficiencies when applied to continuous or non-normally distributed data (Surucu, 2008; Ghasemi and Zahediasl, 2012; Rana and Singhal, 2015; Luong, 2018; Khatun, 2021; Hagel et al., 2024). Consequently, the K-S test provided a more versatile and reliable approach for confirming the suitability of the chosen distribution in this context.

The goodness of fit was confirmed by a K-S statistic, representing the maximum difference between the empirical cumulative distribution function (CDF)[7] and the CDF of the fitted distribution, with values of 0.0031962 (Job 1) and 0.0032078 (Job 4). As these values are below the critical threshold of 0.01, excellent fits are implied. Therefore, it was concluded that the committed equivalent lung dose coefficient was well modelled by a lognormal distribution, with a GM of 47.05 mSv/(mJh/m^3) and a GSD of 1.58 for Job 1. Similarly, the best fit for Job 4 was also a lognormal distribution, with a GM of 61.87 mSv/(mJh/m^3) and a GSD of 1.56.

Having accomplished this, the next step was to perform a sensitivity analysis to identify which groups of parameters have the greatest influence on the calculated committed equivalent dose coefficients for both exposure scenarios. Since the lung dose accounts for at least 95 % of the effective dose following inhalation of radon progeny and was the primary organ of interest in this study, the sensitivity analysis therefore focused on the committed equivalent lung dose coefficient. The results of the sensitivity analysis are presented in the subsequent sections.

4.4. Sensitivity of dose to uncertainty in the different model parameter groups

The sensitivity of the committed equivalent lung dose coefficient to the various parameter groups is presented in this subsection. The results are summarized in Tables 8 and 9 for Jobs 1 and 4, respectively. The analysis was conducted using the Monte Carlo simulation methodology described in Table 2. This methodology quantifies the contribution of each parameter group to the overall uncertainty in the calculated equivalent lung dose coefficient.

[6] The parameter U represents a test statistic used to determine whether there is a significant difference between two independent samples.

[7] CDF is the probability that a continuous random variable has a value less than or equal to a given value.

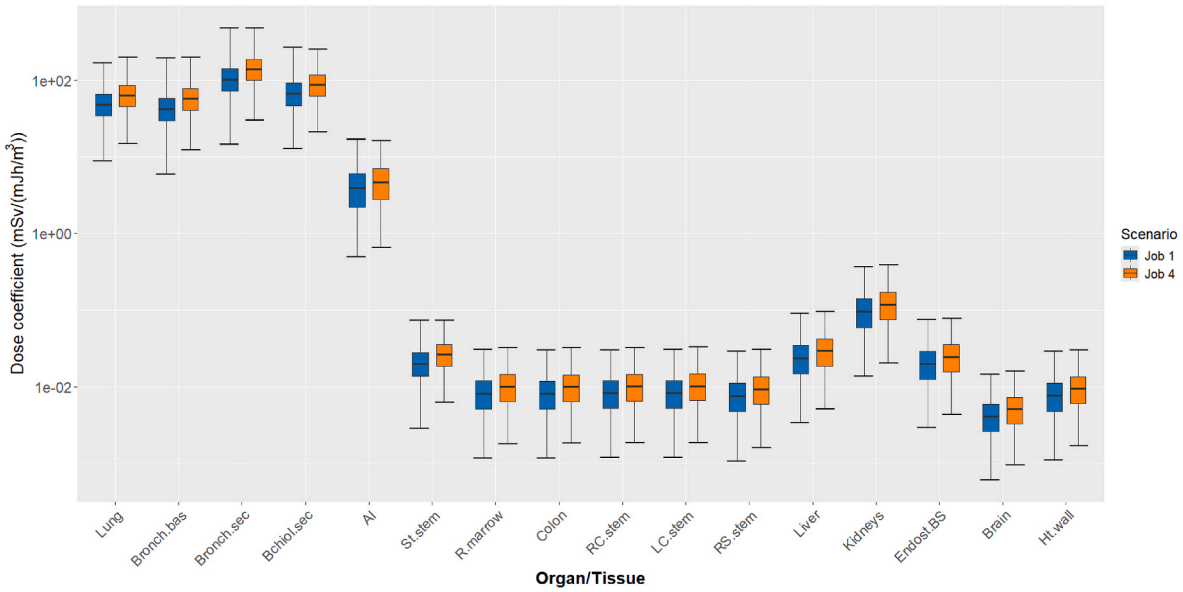

Fig. 4. Boxplots showing the comparison of dose coefficients from the uncertainty analysis due to inhalation of radon progeny in underground mines under Job 1 and Job 4 exposure conditions.

Table 7
Hypothesis testing results from the Mann-Whitney *U* test for the committed equivalent dose coefficients (Job1-Job4) due to inhalation of radon progeny in underground mines.

Organ	U-statistic	p-value	Lower bound	Upper bound	Conclusion
Lung	844108874	0	−16.275306486	−1.563076E+01	Reject H_0
Bronch.bas	800025624	0	−16.353386275	−1.572746E+01	Reject H_0
Bronch.sec	816563681	0	−38.116013687	−3.662982E+01	Reject H_0
Bchiol.sec	861623685	0	−20.865825302	−1.996313E+01	Reject H_0
AI	1054938447	0	−0.812080696	−7.421513E-01	Reject H_0
St.stem	869803862	0	−0.006307882	−6.021458E-03	Reject H_0
R.marrow	996700895	0	−0.001986989	−1.855644E-03	Reject H_0
Colon	991861907	0	−0.001989495	−1.858328E-03	Reject H_0
RC.stem	990531471	0	−0.002012250	−1.888697E-03	Reject H_0
LC.stem	988950724	0	−0.002050828	−1.917849E-03	Reject H_0
RS.stem	1000913275	0	−0.001817771	−1.696854E-03	Reject H_0
Liver	1000498515	0	−0.005704884	−5.340373E-03	Reject H_0
Kidneys	1002141240	0	−0.022924443	−2.148859E-02	Reject H_0
Endost.BS	996742047	0	−0.004839645	−4.523037E-03	Reject H_0
Brain	977350399	0	−0.001036001	−9.760035E-04	Reject H_0
Ht.wall	993880952	0	−0.001869726	−1.753668E-03	Reject H_0

To assess the impact of specific parameter groups, such as absorption parameters, Monte Carlo simulations were conducted using two distinct calculation approaches, as outlined in Table 2. The results from calculation approach (i), in which only the target parameter group was varied while the others were held constant at their ICRP reference values, are presented in the row labelled 'Parameter'. Conversely, the results from calculation approach (ii), where the target parameter group was held constant and all the others were varied, are shown in the corresponding row labelled 'Parameter.other', as described in Section 3.4. The influence of absorption parameters on the committed equivalent lung dose coefficient, for example, is reported under 'Absorption' for approach (i) and 'Absorption.other' for approach (ii) in Tables 8 and 9

4.4.1. Sensitivity of the committed equivalent lung dose coefficient to uncertainty in the activity parameters of the HRTM particle deposition model

The committed equivalent lung dose coefficient resulting from the inhalation of radon progeny in underground mining environments is highly sensitive to activity parameters. These physiological factors determine the quantity and characteristics of air and thus of radioactive aerosols inhaled, thereby directly influencing deposition patterns, dose distribution and the total radiation burden delivered to lung tissues. Their role is even more critical in physically demanding jobs, where elevated respiratory activity can significantly increase the inhaled dose.

The results of the Monte Carlo simulations to assess the contribution of these parameters to the overall uncertainty in the committed equivalent lung dose coefficient indicate that the greatest uncertainty occurs when all parameters are varied simultaneously (UF = 2.37 for Job 1 and 2.32 for Job 4). However, focusing exclusively on activity parameters still results in a substantial UF (2.26 and 2.30 for Jobs 1 and 4, respectively), emphasizing their dominant influence particularly in Job 4, where they account for almost all of the uncertainty.

The physical relevance of these parameters is underscored by their mechanistic links to inhalation dynamics. For instance, increased tidal volume and breathing frequency common in high-exertion roles such as hewing amplify radon progeny intake, resulting in higher lung doses. The nasal fraction also matters; nasal breathing partially filters out aerosols, whereas mouth breathing allows greater penetration of radon progeny into the lungs. Therefore, changes in breathing patterns due to exertion or environmental factors (e.g., heat or poor ventilation as is the case in Job 4) increase dose uncertainty.

Notably, the lower UF observed when only 'Activity.other' parameters are varied (1.26 for Job 1 and 1.05 for Job 4) demonstrate that,

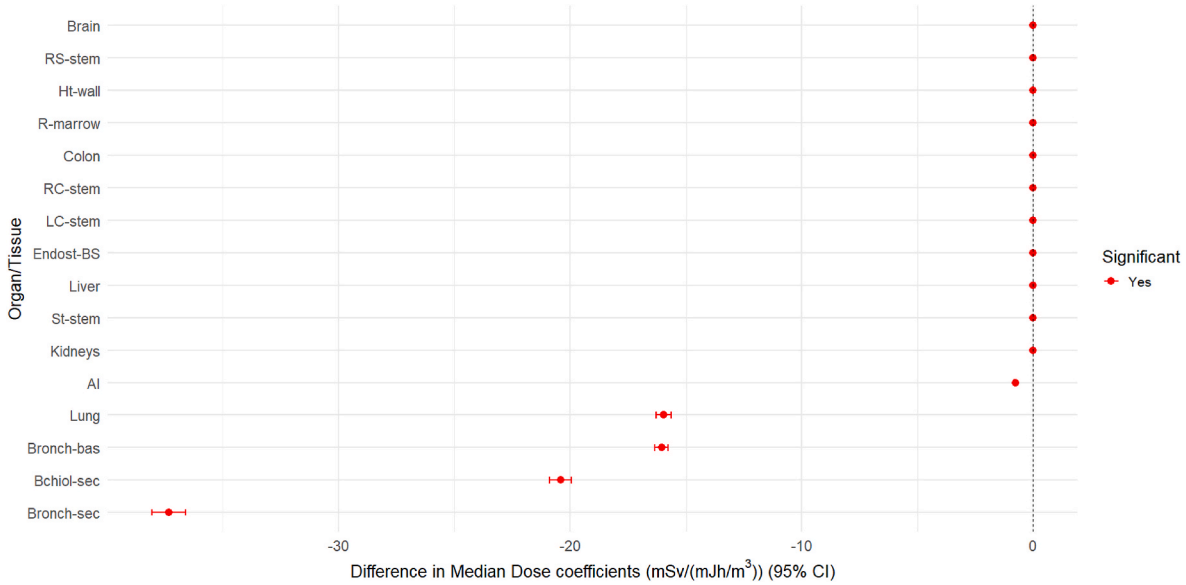

Fig. 5. Forest plot showing hypothesis testing results for the comparison of committed equivalent dose coefficients (Job1-Job4) using Mann-Whitney *U* test due to inhalation of radon progeny in underground mines.

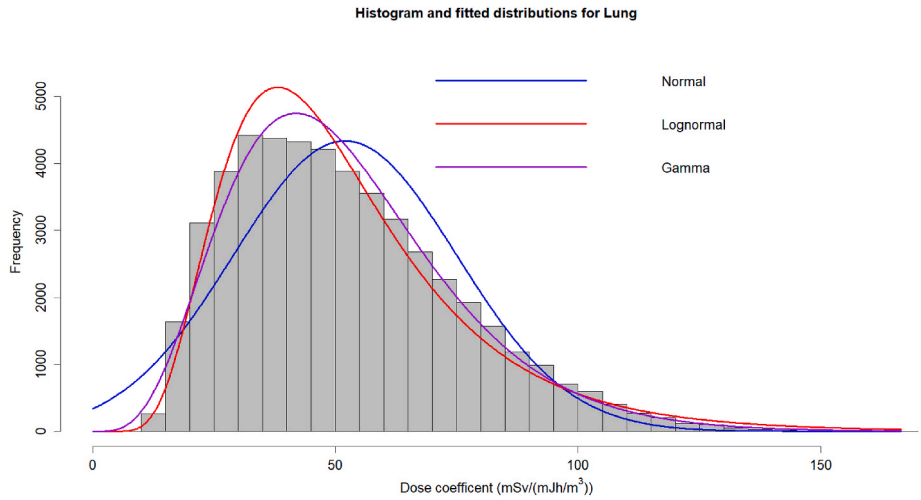

Fig. 6. Histogram and fitted posterior distributions to the committed equivalent lung dose coefficient (mSv/(mJh/m^3)) from the inhalation of radon progeny in underground mines under Job 1 exposure conditions.

although other inputs contribute to the dose, activity parameters are more influential. However, dose outcomes are also affected by environmental differences, such as variations in radon progeny concentration and aerosol characteristics between jobs. This confirms that, although activity parameters are important, they must be considered in the context of job-specific environmental exposures.

4.4.2. Sensitivity of the committed equivalent lung dose coefficient to uncertainty in the aerosol parameters of the HRTM particle deposition model

Aerosol parameters have a significant impact on particle deposition in the respiratory tract and consequently on dose estimates for radon progeny inhalation in underground mining environments. Monte Carlo simulations were used to assess the sensitivity of the committed equivalent lung dose coefficient to aerosol parameters for Jobs 1 and 4.

In Job 1, the presence of smaller, less stable particles and fluctuating unattached fractions significantly impacts dose variation due to aerosol parameters. This is reflected in a GSD of 1.12 and UF of 1.25). When all other parameters except aerosols ('Aerosol.other') are varied, the UF increases to 1.56, indicating interactive effects and highlighting the importance of aerosol behavior in dose assessments. By contrast, Job 4 exhibits a highly stable aerosol environment with minimal sensitivity to variation in the aerosols (both GSD and UF = 1.01). In this case, most of the dose uncertainty originates from 'Aerosol.other' parameters, with a UF of 2.32 that matches the overall UF.

Despite higher radon progeny activity concentrations, the consistent aerosol properties in Job 4 lead to narrower dose ranges and more predictable lung doses. The unattached fraction remains the primary aerosol variable, but its impact is relatively minor compared to the influence of activity parameters and exposure conditions. These findings suggest that, in Job 1, aerosol parameters alone contribute less to the overall uncertainty in the committed equivalent lung dose coefficient, while in Job 4, their contribution is negligible.

4.4.3. Sensitivity of the committed equivalent lung dose coefficient to uncertainty in the subject parameters of the HRTM particle deposition model

Subject parameters influence aerosol deposition by modulating airflow dynamics within the respiratory tract. The sensitivity analysis results for Job 1 show that varying only the subject parameters yielded a

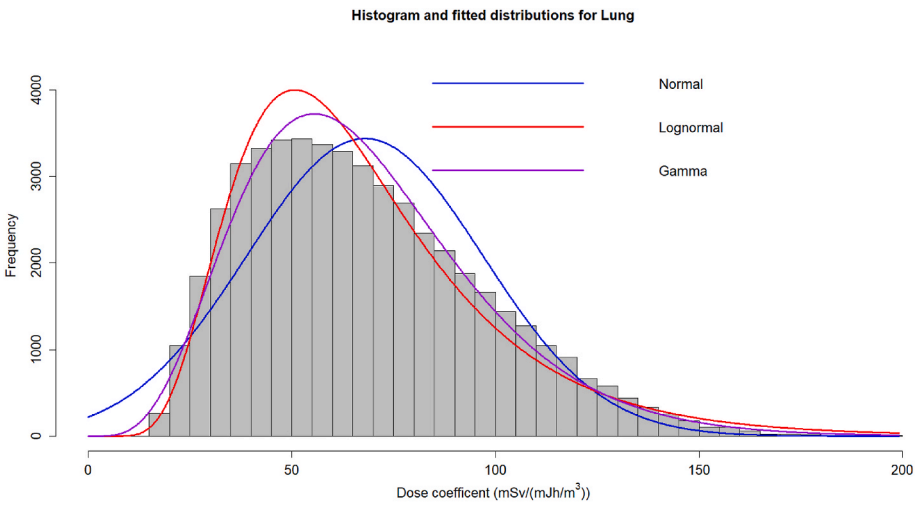

Fig. 7. Histogram and fitted posterior distributions to the committed equivalent lung dose coefficient (mSv/(mJh/m^3)) from the inhalation of radon progeny in underground mines under Job 4 exposure conditions.

Table 8
Statistical summary of the comparison of the sensitivity of the committed equivalent lung dose coefficient (mSv/(mJh/m^3)) to parameter groups from inhalation of radon progeny in underground mines under Job 1 exposure conditions.

Parameters	Median	Mean	GM	Q_L	Q_U	SD	GSD	UF
All	48.44	52.01	47.05	18.59	104.74	23.00	1.58	2.37
Activity	40.69	43.09	39.04	16.13	82.68	17.95	1.55	2.26
Activity.other	38.43	38.44	38.17	29.92	47.63	4.56	1.13	1.26
Aerosol	37.18	37.27	36.93	29.04	45.55	4.31	1.12	1.25
Aerosol.other	42.52	45.16	41.14	16.75	87.14	19.04	1.56	1.56
Subject	34.75	34.77	34.73	32.78	36.66	1.10	1.03	1.06
Subject.other	47.29	50.75	46.00	18.42	101.48	22.24	1.57	2.35
Absorption	33.81	33.81	33.81	33.59	34.04	0.15	1.01	1.01
Absorption.other	47.55	50.97	46.19	18.45	102.18	22.34	1.57	2.35
Particle transport	33.54	33.54	33.54	33.15	33.91	0.21	1.01	1.01
Particle transport.other	48.55	52.19	47.25	18.74	104.60	22.91	1.58	2.36

GM: Geometric mean; GSD: Geometric standard deviation; SD: Standard deviation; UF: Uncertainty factor; Q_L: 2.5th percentile; Q_U: 97.5th percentile.

Table 9
Statistical summary of the comparison of the sensitivity of the committed equivalent lung dose coefficient (mSv/(mJh/m^3)) to parameter groups from inhalation of radon progeny in underground mines under Job 4 exposure conditions.

Parameters	Median	Mean	GM	Q_L	Q_U	SD	GSD	UF
All	63.73	67.98	61.87	24.83	133.09	28.98	1.56	2.32
Activity	61.81	65.96	60.05	24.35	129.30	28.12	1.56	2.30
Activity.other	47.02	47.03	47.00	44.70	49.30	1.25	1.03	1.05
Aerosol	45.61	45.62	45.61	45.00	46.26	0.41	1.01	1.01
Aerosol.other	63.28	67.45	61.32	24.52	132.29	28.90	1.56	2.32
Subject	46.50	46.51	46.49	44.56	48.41	1.11	1.02	1.04
Subject.other	62.44	66.51	60.55	24.42	130.27	28.32	1.56	2.31
Absorption	45.71	45.71	45.71	45.43	46.00	0.19	1.01	1.01
Absorption.other	63.29	67.51	61.43	24.71	132.21	28.79	1.56	2.31
Particle transport	45.34	45.35	45.34	44.59	46.08	0.40	1.01	1.02
Particle transport.other	63.84	68.08	61.96	24.84	133.53	29.02	1.56	2.32

GM: Geometric mean; GSD: Geometric standard deviation; SD: Standard deviation; UF: Uncertainty factor; Q_L: 2.5th percentile; Q_U: 97.5th percentile.

median lung dose of 34.75 mSv/(mJh/m^3), which is well below 48.44 mSv/(mJh/m^3) obtained when all parameters were varied and lower than 47.29 mSv/(mJh/m^3) observed when subject parameters were fixed ('Subject.other'). A comparable pattern emerged in Job 4, where the median dose was 46.50 mSv/(mJh/m^3) for subject-only variation versus 63.73 mSv/(mJh/m^3) for all parameters varied and 62.44 mSv/(mJh/m^3) for 'Subject.other'. These lower median, mean and GM values suggest that subject parameters contribute minimally to central dose estimates.

Uncertainty metrics reinforce this finding. For instance in Job 1, the standard deviation (SD),[8] and UF for subject-only variation were low at 1.10 mSv/(mJh/m^3) and 1.06 respectively, compared to 23.00 mSv/

[8] As a measure of variation, SD determines how much the data values deviate from the mean or the closeness of a particular data structure from the mean (Mbaji et al., 2023).

(mJh/m^3) and a UF of 2.37 for all parameter variation. Similar trends were observed in Job 4, with an even lower UF of 1.04 for subject parameters. These results confirm that 'Subject.other' parameters are the main sources of dose uncertainty, particularly in settings involving high exposure, such as Job 4.

Interestingly, subject parameters had a slightly greater impact at the lower end of the dose distribution. For example, in Job 1, Q_L was 32.78 mSv/(mJh/m^3) for subject-only variation, which is notably higher than 18.59 mSv/(mJh/m^3) and 18.42 mSv/(mJh/m^3) observed for all parameters and 'Subject.other' parameters. This suggests that subject parameter variation slightly increases minimum dose estimates. However, these parameters had little effect on Q_U values, which remained low in contrast to the much higher extremes observed for 'Subject.other'. From a physiological perspective, this is to be expected, given that V_D affects upper-airway deposition and therefore contributes minimally to total dose.

4.5. Sensitivity of the committed equivalent lung dose coefficient to uncertainty in absorption parameters

Absorption parameters describe the rate at which inhaled radioactive particles, particularly radon progeny, transfer from the respiratory tract to the bloodstream. Sensitivity analysis results show that the median lung dose when absorption parameters are varied alone is 33.81 mSv/(mJh/m^3) for Job 1, which is substantially lower than the 48.44 mSv/(mJh/m^3) observed when all parameters are varied. Similarly, Job 4 exhibits a comparable pattern i.e. 45.71 mSv/(mJh/m^3) for absorption only variation versus 63.73 mSv/(mJh/m^3) for all-parameter variation. This trend reflects the limited sensitivity of lung dose estimates to variation in the absorption rates.

Uncertainty metrics further support this observation. For both jobs, the SD is extremely low i.e. 0.15 mSv/(mJh/m^3) for Job 1 and 0.19 mSv/(mJh/m^3) for Job 4. The GSD and UF are both 1.01 in each case, indicating that the dose outcome remains almost constant regardless of absorption rate fluctuation. The narrow percentile range, particularly in Job 1 (Q_L = 33.59 mSv/(mJh/m^3), Q_U = 34.04 mSv/(mJh/m^3)), highlights the stability and predictability of dose estimates based on absorption parameters alone.

However, when all parameters except absorption are varied, the uncertainty profile closely mirrors that of the full-parameter simulation. In Job 1, the median dose for 'Absorption.other' is 47.55 mSv/(mJh/m^3), with a UF of 2.35 nearly identical to the UF of 2.37 for the full-parameter simulation. Job 4 shows a similar result (UF = 2.31 for 'Absorption.other' versus 2.32 for all parameters). These results clearly indicate that the dominant sources of dose uncertainty lie outside the absorption domain. While these parameters are biologically significant for internal dosimetry, they demonstrate minor variation and influence on lung dose uncertainty for the case of radon progeny inhalation.

4.6. Sensitivity of the committed equivalent lung dose coefficient to uncertainty in particle transport parameters

The movement and deposition of inhaled radioactive aerosols within the respiratory tract is governed by particle transport parameters. The sensitivity analysis results for Job 1 show that, the committed equivalent lung dose coefficient associated with variation in these parameters is notably lower at a median of 33.54 mSv/(mJh/m^3) compared to 48.44 mSv/(mJh/m^3) when all parameters are varied. Similarly, in Job 4, the median dose is 45.34 mSv/(mJh/m^3) for particle transport variation alone versus 63.73 mSv/(mJh/m^3) for the full parameter scenario. These substantial differences highlight the limited contribution of particle transport to overall dose sensitivity.

Uncertainty metrics support this interpretation. The SD for particle transport in Job 1 is just 0.21mSv/(mJh/m^3), with a GSD and UF of 1.01 indicating extremely tight dose distributions. Job 4 shows slightly broader but still low uncertainty (SD = 0.40 mSv/(mJh/m^3), GSD = 1.01, UF = 1.02). These values confirm that, although particle transport parameters are integral to deposition modelling, they have a minimal effect on propagated uncertainty under job-specific conditions.

Conversely, when all parameters except particle transport are varied ('Particle transport.other'), the uncertainty is close to that of the full-parameter case. For instance, Job 1 exhibits a UF of 2.36 and 2.37 for all parameters, whereas Job 4 maintains a UF of 2.32 in both instances. This highlights that most dose uncertainty arises from other sources. Despite their biophysical relevance, sensitivity analysis results show that variation in particle transport parameters alone introduces minor variation to estimates of committed equivalent lung dose coefficient.

The sensitivity analysis results for this subsection are also presented in form of grouped boxplots in Fig. 8 for Job 1 and Job 4 inclusive for a graphical visualization.

Since the results presented in Tables 8 and 9 indicate that the committed equivalent lung dose coefficient is most sensitive to the activity parameters of the HRTM deposition model, further sensitivity studies were done to identify which of these activity parameters had the greatest influence on the committed equivalent lung dose coefficient. The results are presented in the subsequent sections.

4.7. Sensitivity of the committed equivalent lung dose coefficient to uncertainty in the activity parameters of the HRTM particle deposition model

This section examines how sensitive the committed equivalent lung dose coefficient is to individual activity parameters. Detailed results for Jobs 1 and 4 are provided in Tables 10 and 11, respectively. The same Monte Carlo simulation methodology described in Table 2 was employed for the analysis, as was used in the previous subsection. However, unlike the previous analysis, which assessed grouped parameters, this subsection focuses on the influence of individual activity parameters. This approach enables more precise quantification of the contribution of each parameter to overall uncertainty in the calculated committed equivalent lung dose coefficient.

4.7.1. Sensitivity of the committed equivalent lung dose coefficient to uncertainty in breathing frequency

The sensitivity analysis of the committed equivalent lung dose coefficient shows that breathing frequency has a smaller effect on the committed equivalent lung dose coefficient compared to activity parameters and 'Breathing frequency.other' parameters.

For both Job 1 and Job 4, the median and mean values for breathing frequency are consistently lower. For Job 1, the values (32.01 mSv/(mJh/m^3) and 32.04 mSv/(mJh/m^3)) are significantly lower than those for activity parameters (40.69 mSv/(mJh/m^3) and 43.09 mSv/(mJh/m^3)) and 'Breathing frequency.other' parameters (44.92 mSv/(mJh/m^3) and 45.39 mSv/(mJh/m^3)). A similar trend can be observed for Job 4. The GM also confirms the lower effect of breathing frequency.

Variation metrics, including SD, GSD and UF (6.66 mSv/(mJh/m^3), 1.24 and 1.43 respectively), indicate that dose contributions from breathing frequency are more stable and predictable. This suggests that breathing frequency alone contributes less to committed equivalent lung dose coefficient when compared to 'Breathing frequency.other' parameters.

4.7.2. Sensitivity of the committed equivalent lung dose coefficient to uncertainty in the fraction of air breathed through the nose

The sensitivity analysis of the committed equivalent lung dose coefficient highlights the role of the nasal fraction in reducing lung exposure compared to activity and 'Nasal fraction.other' parameters. For Job 1, the median and mean dose values for the nasal fraction are consistently lower, indicating its effectiveness in filtering radioactive particles. For instance, the median and mean values (34.77 mSv/(mJh/m^3) and 34.89 mSv/(mJh/m^3)) are significantly lower than those for activity parameters (40.69 mSv/(mJh/m^3) and 43.09 mSv/(mJh/m^3))

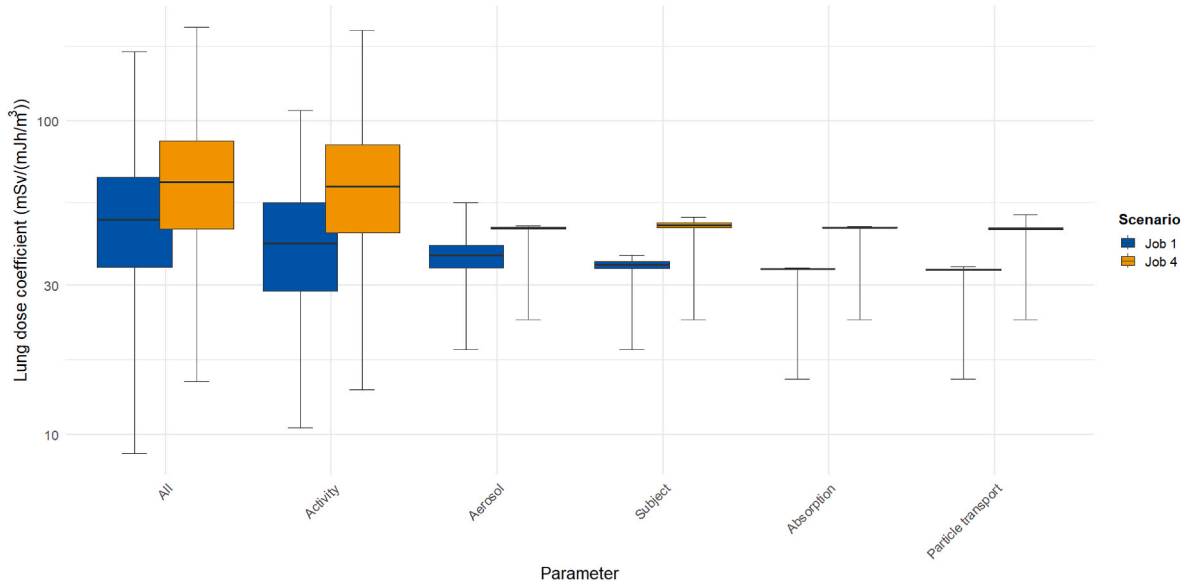

Fig. 8. Grouped boxplots showing sensitivity of committed equivalent lung dose coefficient to parameter groups under Job 1 and Job 4 exposure conditions.

Table 10
Statistical summary of the comparison of the sensitivity of the committed equivalent lung dose coefficient (mSv/(mJh/m^3)) to different activity parameters from inhalation of radon progeny in underground mines under Job 1 exposure conditions.

Parameters	Median	Mean	GM	Q_L	Q_U	SD	GSD	UF
Activity	40.69	43.09	39.04	16.13	82.68	17.95	1.55	2.26
Breathing frequency	32.01	32.04	31.33	21.09	42.99	6.66	1.24	1.43
Breathing frequency.other	44.92	45.39	42.36	19.75	75.21	16.07	1.47	1.95
Nasal fraction	34.77	34.89	34.88	33.70	36.63	0.84	1.02	1.04
Nasal fraction.other	39.37	41.71	38.05	15.56	79.94	17.44	1.55	2.26
Tidal volume	43.32	43.53	40.73	19.23	68.58	15.01	1.46	1.89
Tidal volume.other	33.25	33.46	32.62	21.05	47.67	7.42	1.26	1.51
Time fraction	33.68	33.69	33.58	29.35	38.02	2.63	1.08	1.14
Time fraction.other	40.82	42.93	39.32	16.32	81.12	17.51	1.54	2.23

GM: Geometric mean; GSD: Geometric standard deviation; SD: Standard deviation; UF: Uncertainty factor; Q_L: 2.5th percentile; Q_U: 97.5th percentile.

Table 11
Statistical summary of the comparison of the sensitivity of the committed equivalent lung dose coefficient (mSv/(mJh/m^3)) to different activity parameters from inhalation of radon progeny in underground mines under Job 4 exposure conditions.

Parameters	Median	Mean	GM	Q_L	Q_U	SD	GSD	UF
Activity	61.81	65.96	60.05	24.35	129.30	28.12	1.56	2.30
Breathing frequency	43.30	43.34	42.31	28.23	58.22	9.09	1.24	1.44
Breathing frequency.other	67.72	69.20	64.49	29.76	119.64	25.02	1.47	2.01
Nasal fraction	52.83	53.79	53.48	45.76	66.39	5.87	1.11	1.21
Nasal fraction.other	52.73	55.76	51.05	21.32	105.84	22.88	1.54	2.23
Tidal volume	57.92	58.13	54.63	26.55	90.37	19.41	1.44	1.85
Tidal volume.other	50.60	51.61	49.98	30.49	79.06	13.01	1.29	1.61
Time fraction	45.54	45.55	45.39	39.40	51.71	3.75	1.09	1.15
Time fraction.other	61.77	65.70	60.02	24.61	125.88	27.36	1.55	2.26

GM: Geometric mean; GSD: Geometric standard deviation; SD: Standard deviation; UF: Uncertainty factor; QL: 2.5th percentile; QU: 97.5th percentile.

and 'Nasal.other' parameters (39.37 mSv/(mJh/m^3) and 41.71 mSv/(mJh/m^3)).

The variation metrics confirm this trend. For instance, the nasal fraction has SD, GSD and UF values indicating greater stability. For instance, the SD for Job 1 is 0.84 mSv/(mJh/m^3), significantly lower than the activity parameters (17.95 mSv/(mJh/m^3)). Similarly, the UF for the nasal fraction is much lower, reinforcing its predictability.

For Job 4, although the parameter values increase, they remain lower than the values associated with the activity parameters. This suggests that poor air quality in Job 4 likely prompts miners to breathe through their mouths, bypassing the natural filtration system of nasal breathing. Consequently, more radon progeny can penetrate deeper into the lungs, exposing sensitive lung tissues to increased radiation and thereby elevating the risk of lung cancer.

These findings suggest that nasal fraction alone has a minor contribution to the committed equivalent lung dose coefficient in Job 1 and minimal contribution in Job 4.

4.7.3. Sensitivity of the committed equivalent lung dose coefficient to uncertainty in tidal volume

The sensitivity analysis of the committed equivalent lung dose coefficient shows that tidal volume has a significant influence on exposure. Its values are consistently higher than those for 'Tidal volume.other'. For instance, the results for Job 1 show that the median and mean values for

tidal volume (43.32 mSv/(mJh/m^3) and 43.53 mSv/(mJh/m^3)) are higher than those for 'Tidal volume.other' parameters (33.25 mSv/(mJh/m^3) and 33.46 mSv/(mJh/m^3)). A similar pattern is observed for Job 4, where tidal volume values (57.92 mSv/(mJh/m^3) and 58.13 mSv/(mJh/m^3)) exceed 'Tidal volume.other' parameters.

The GM, GSD and UF follow the same trend, emphasizing the influence of tidal volume on the committed equivalent lung dose coefficient. The results suggest that increased depth of breathing increases the risk of exposure, particularly in physically demanding or poorly ventilated environments. This suggests that tidal volume alone makes a significant contribution to the committed equivalent lung dose coefficient when compared to 'Tidal volume.other' parameters.

4.7.4. Sensitivity of the committed equivalent lung dose coefficient to uncertainty in the fraction of time spent in each activity

The sensitivity analysis of the committed equivalent lung dose coefficient shows that the time fraction has a stable and predictable effect on lung exposure, with consistently lower dose coefficients and reduced uncertainty compared to activity and 'Time fraction.other' parameters.

For both Job 1 and Job 4, the median and mean values for the time fraction are significantly lower. For Job 1, the median and mean values (33.68 mSv/(mJh/m^3) and 33.69 mSv/(mJh/m^3)) are lower than those for activity parameters (40.69 mSv/(mJh/m^3) and 43.09 mSv/(mJh/m^3)). Similarly, for Job 4, the values for the time fraction (45.54 mSv/(mJh/m^3) and 45.55 mSv/(mJh/m^3)) remain lower than those for the activity parameters (61.81 mSv/(mJh/m^3) and 65.96 mSv/(mJhm^{-3})).

The time fraction also shows lower uncertainty, as indicated by its lower SD, GSD and UF values. For Job 1, the SD is 2.63 mSv/(mJh/m^3), significantly lower than for the activity parameters (17.95 mSv/(mJh/m^3)).These results suggest that while time fraction has a minimal effect on lung dose coefficients, prolonged exposure combined with high intensity activity could increase risks.

In summary, sensitivity analysis of the committed equivalent lung dose coefficient shows that tidal volume has the greatest influence on lung dose, while breathing frequency, nasal fraction and time fraction have comparatively less effects. Tidal volume is particularly important because deeper breaths lead to an increased deposition of radioactive particles in the lungs. This is reflected in the consistently higher GSD and UF values for tidal volume compared to other parameters, which highlights its critical role in exposure risk.

In contrast, breathing frequency contributes less to lung dose since it does not significantly affect inhalation depth. The nasal fraction mitigates exposure by filtering more radioactive particles during nasal breathing than oral breathing, thereby reducing dose coefficients. Time fraction also has a limited impact since it is not directly related to breathing depth or the intensity of physical activity. However, prolonged exposure combined with high-intensity activities can still elevate the lung dose.

These findings highlight the need to prioritise radiation protection strategies targeting tidal volume, the main contributor to lung dose. Key measures include improved ventilation, time restrictions in high-exposure zones, respiratory protection, encouraging nasal breathing, and optimizing work/rest cycles to reduce risks and enhance worker safety in contaminated environments.

A graphical representation of the above results in form of grouped boxplots is also given in Fig. 9 for Job 1 and Job 4 inclusive.

5. Conclusion

This study evaluated the uncertainties associated with committed equivalent dose coefficients from the inhalation of radon progeny in underground mining environments. Specifically, it compared two occupational scenarios derived from the former Wismut uranium mines. Job 1 involved wet drilling with good ventilation, while Job 4 involved dry drilling with poor ventilation. The analysis revealed that Job 4 mining operations produced significantly higher lung dose coefficients up to 1.6 times higher than Job 1 suggesting substantially elevated risks of radiation-induced health effects, particularly lung cancer. Although the dose coefficients in Job 4 were significantly higher than in Job 1, the uncertainties in these values were similar. Uncertainty analysis results revealed that substituting Job 4 conditions with those of Job 1 demonstrated the potential for reducing lung dose coefficients by around 36 %, highlighting the critical impact of ventilation and dust suppression.

The Bronch.sec region of the lungs consistently received the highest doses in both scenarios, indicating that this is the most likely site for the development of radon-induced malignancies. Outside the lungs, the kidneys received the greatest dose among systemic organs. While not highly radiosensitive, the kidneys may still be affected by the chemical toxicity of radon progeny, which warrants attention in occupational health assessments. Of all the lung regions, the AI region showed the greatest uncertainty. Similarly, the kidneys showed the greatest uncertainty among systemic tissues.

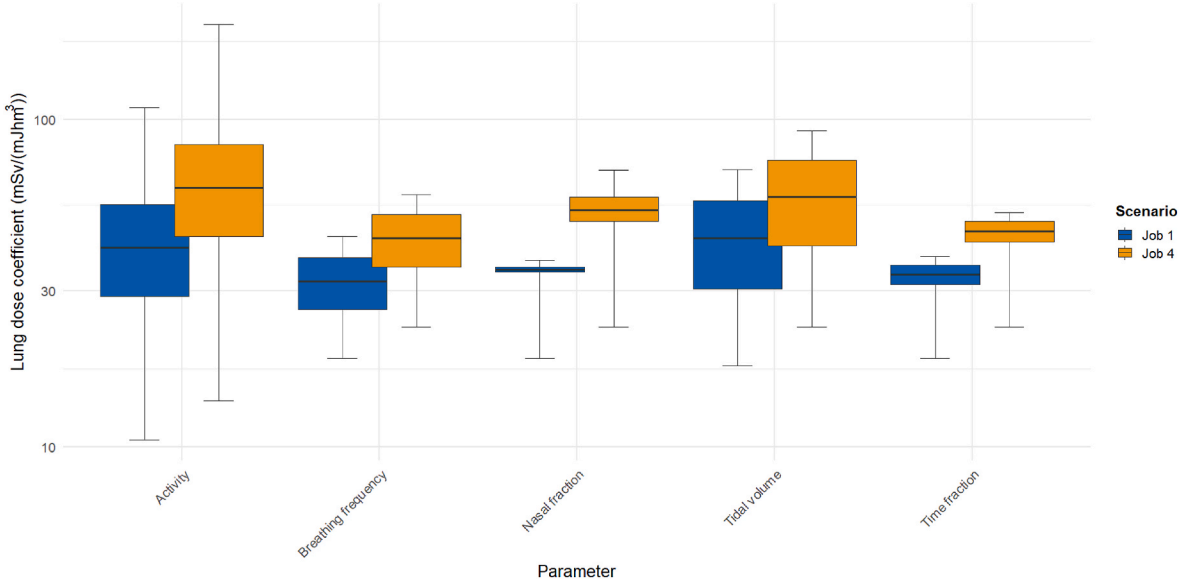

Fig. 9. Grouped boxplots showing the sensitivity of the committed equivalent lung dose coefficient (mSv/(mJh/m^3)) to activity parameters under Job 1 and Job 4 exposure conditions.

Uncertainty analysis indicated that the dose coefficients for both job types followed lognormal distributions with substantial positive skew, resulting in wide confidence intervals. For Job 1, the 95 % confidence interval ranged from 18.59 to 104.74 mSv/(mJh/m^3) and for Job 4 from 24.83 to 133.09 mSv/(mJh/m^3). Both sets of results exceeded the ICRP reference value of 24.00 mSv/(mJh/m^3) by at least a factor of two. This suggests that relying solely on reference values for dose assessment could lead to a significant underestimation of the actual lung dose received by miners, particularly in conditions involving high exposure, such as those of Job 4.

Furthermore, a statistical comparison using the Mann–Whitney *U* test confirmed that the two job scenarios had significantly different exposure profiles and dose distributions. The test returned p-values close to zero for all organs and tissues, well below the 0.05 significance threshold. This rejects the null hypothesis and confirms that the dose coefficients are distributed differently between Jobs 1 and 4. This statistical evidence highlights the need for job-specific radiological protection measures.

The sensitivity analysis revealed that tidal volume had the greatest influence on dose coefficient uncertainty among the parameters. Deeper breaths facilitate greater deposition of radioactive particles in the lungs, making tidal volume a critical determinant of internal dose. In contrast, other parameters such as breathing frequency, nasal fraction and time fraction played a comparatively lesser role. These findings emphasize the importance of using refined, realistic parameter values in exposure modelling to reduce uncertainty in dose estimates.

Taken together, these findings highlight the importance of refining operational and regulatory approaches to occupational radiation protection. Improving ventilation in underground mines emerges as a key intervention. The significant reduction in dose coefficients observed under Job 1 conditions shows that well-ventilated environments can greatly reduce radon progeny concentrations and related health risks. From an operational perspective, controlling work practices to minimize time spent in high-exposure zones is also crucial. Optimizing work-rest cycles, particularly during physically demanding tasks, can help limit the inhalation of radon progeny aerosols due to deeper breathing.

Where physical activity in high-exposure areas is unavoidable, the consistent use of respiratory protective equipment must be mandatory. Respirator standards must reflect the elevated dose coefficients identified in this study to ensure adequate protection. Additionally, continuous air monitoring in active workspaces should be standard practice to capture fluctuations in radon progeny concentrations and inform real-time protective responses.

From a regulatory perspective, there is a compelling case for revising the reference dose coefficients and action levels in order to account for the wide uncertainty ranges revealed in this study. Using higher percentiles of the dose distribution, such as the 75^{th} or 95^{th}, or adopting mean dose values from probabilistic simulations, could yield more conservative and realistic exposure guidelines. Updating biokinetic models to include more accurate, scenario-specific activity parameters would further improve the accuracy and reliability of dose assessments.

CRediT authorship contribution statement

Thomas Makumbi: Visualization, Software, Investigation, Data curation, Writing – review & editing, Conceptualization, Writing – original draft, Validation, Methodology, Formal analysis. **Bastian Breustedt:** Supervision, Writing – review & editing, Software, Conceptualization, Methodology. **Wolfgang Raskob:** Resources, Funding acquisition, Writing – review & editing, Project administration. **Sadeeb Simon Ottenburger:** Writing – review & editing, Project administration, Resources.

Declaration of competing interest

The authors declare that they have no known competing financial interests or personal relationships that could have appeared to influence the work reported in this paper.

Acknowledgements

The authors gratefully acknowledge the vital contributions of Dr. James Marsh, Dr. Vladimir Spielmann, Dr. Edilaine Honorio da Silva, and Dr. David Broggio to the successful completion of this work. They further recognize the support of the state of Baden-Württemberg through the bwHPC initiative. Lastly, this work received funding from the Euratom Research and Training Programme 2019–2020 under Grant Agreement No. 900009 (RadoNorm).

Data availability

Data will be made available on request.

References

Aslam, M., 2019. Introducing Kolomogorov-Smirnov tests under uncertainty: an application to radioactive data. ACS Omega Publications 5 (1), 914–917. https://doi.org/10.1021/acsomega.9b03940.

Booker, D.V., Chamberlain, A.C., Newton, D., Stott, A.N., 1969. Uptake of radioactive lead following inhalation and injection. Br. J. Radiol. 42 (498), 457–466. https://doi.org/10.1259/0007-1285-42-498-457.

Boudene, C., Malet, D., Masse, R., 1977. Fate of ^{210}Pb inhaled by rats. Toxicol. Appl. Pharmacol. 41 (2), 271–276. https://doi.org/10.1016/0041-008X(77)90027-8.

Breustedt, B., Blanchardon, E., Castellani, C.M., Etherington, G., Franck, D., Giussani, A., Hofmann, W., Lebacq, A.L., Li, W.B., Noßke, D., Lopez, M.A., 2017. EURADOS work on internal dosimetry. Ann. ICRP 47 (3–4), 75–82. https://doi.org/10.1177/0146645318756232.

Breustedt, B., Giussani, A., Noßke, D., 2018. Internal dose assessment - concepts, models and uncertainties. Radiat. Meas. 115, 49–54. https://doi.org/10.1016/jradmeas201806013.

Breustedt, B., Chavan, N., Makumbi, T., 2024. An R code for calculation of dose coefficients and studying their uncertainties. Health Physics. Manuscript accepted for publication. https://doi.org/10.1097/HP.0000000000001833.

Butterweck, G., Schuler, Ch, Vezzu, G., Müller, R., Marsh, J.W., Thrift, S., Birchall, A., 2002. Experimental determination of the absorption rate of unattached radon progeny from respiratory tract to blood. Radiat. Protect. Dosim. 102 (4), 343–348. https://doi.org/10.1093/oxfordjournals.rpd.a006103.

Cardoso, D.O., Galeno, T.D., 2023. Online evaluation of the Kolmogorov-Smirnov test on arbitrarily large samples. J. Comput. Sci. 67, 101959. https://doi.org/10.1016/j.jocs.2023.101959.

Chamberlain, A.C., Heard, M.J., Little, P., Newton, D., Wells, A.C., Wiffen, R.D., 1978. Investigations into lead from motor vehicles. UK Atomic Energy Authority Report AERE-R 9198. HMSO, London.

Chen, J., 2023. A review of radon exposure in non-uranium mines: estimation of radon exposure in Canadian mines. Health Phys. 124 (4), 244–256. https://doi.org/10.1097/HP.0000000000001661.

Diogo, M.T., 2020. European legal framework related to underground mining and tunnelling concerning commission directive (EU) 2017/164, 31 January establishing a fourth list of indicative occupational exposure limit values. Int. J. Min. Sci. Technol. 30 (4), 541–545. https://doi.org/10.1016/j.ijmst.2020.05.017.

Ghasemi, A., Zahediasl, S., 2012. Normality tests for statistical analysis. A guide for non-statisticians. Int. J. Endocrinol. Metabol. 10 (2), 486–489. https://doi.org/10.5812/ijem.3505.

Ghorbani, Y., Nwaila, G.T., Zhang, S.E., Bourdeau, J.E., Canovas, M., Arzua, J., Nikadat, N., 2023. Moving towards deep underground mineral resources: drivers, challenges and potential solutions. Resour. Policy 80, 103222. https://doi.org/10.1016/j.resourpol.2022.103222.

Greenhalgh, J.R., Birchall, A., James, A.C., Smith, H., Hodgson, A., 1982. Differential retention of ^{212}Pb ions and insoluble particles in nasal mucosa of the rat. Phys. Med. Biol. 27 (6), 837–851. https://doi.org/10.1088/0031-9155/27/6/005.

Grosche, B., Kreuzer, M., Kreisheimer, M., Schnelzer, M., Tschense, A., 2006. Lung cancer risk among German male uranium miners: a cohort study, 1946–1998. Br. J. Cancer 95, 1280–1287. https://doi.org/10.1038/sj.bjc.6603403.

Hagel, M.L., Trutzenberg, F., Eid, M., 2024. Applying the robust Chi-squared goodness-of-fit test to multilevel multitrait-multimethod models: a Monte Carlo simulation study on statistical performance. Psychology Intern. 6, 462–491. https://doi.org/10.3390/psycholint6020029.

Hoffman, F.O., et al., 2007. Assessing radiological risk in uranium mines. Health Phys. 92 (1), 1–10. https://doi.org/10.1097/01.HP.0000248114.79335.9d.

Hu, J., Iwaoka, K., Hosoda, M., Tokonami, S., 2020. Lung dose estimation of ^{222}Rn and ^{220}Rn progeny based on IMBA Professional Software. Radiat. Environment Medicine 9 (1), 21–27. https://doi.org/10.51083/radiatenvironmed.9.1_21.

Hursh, J.B., Mercer, T.T., 1970. Measurement of ^{212}Pb loss rate from human lungs. J. Appl. Physiol. 28 (3), 268–274. https://doi.org/10.1152/jappl.1970.28.3.268.

Hursh, J.B., Schraub, A., Sattler, E.L., Hofmann, H.P., 1969. Fate of 212-Pb inhaled by human subjects. Health Physics 16 (3), 257–267. https://doi.org/10.1097/00004032-196903000-00001.
ICRP, 1993. Protection against radon-222 at home and at work. ICRP publication 65. Ann. ICRP 23 (2). https://doi.org/10.1177/014664539302300202.
ICRP, 1994. Human respiratory tract model for radiological protection. ICRP publication 66. Ann. ICRP 24 (1–3). https://doi.org/10.1016/0146-6453(94)90029-9.
ICRP, 2006. Human alimentary tract model for radiological protection. ICRP Publication 100. Ann. ICRP 36 (1–2). https://doi.org/10.1016/j.icrp.2006.03.001.
ICRP, 2015. Occupational intakes of radionuclides: part 1. ICRP publication 130. Ann. ICRP 44 (2). https://doi.org/10.1177/0146645315577539.
ICRP, 2017. Occupational intakes of radionuclides: part 3. ICRP publication 137. Ann. ICRP 46 (3/4). https://doi.org/10.1177/0146645317734963.
James, A.C., Greenhalgh, J.R., Smith, H., 1977. Clearance of ^{212}Pb ions from rabbit bronchial epithelium to blood. Phys. Med. Biol. 22 (5), 932–948. https://doi.org/10.1088/0031-9155/22/5/013.
Khatun, N., 2021. Applications of normality test in statistical analysis. Open J. Stat. 11, 113–122. https://doi.org/10.4236/ojs.2021.111006.
Klein, W., Breustedt, B., Urban, M., 2010. Analysis of the variability of biokinetic model parameters due to inter-individual variation. Health Phys. 99 (4), 577–580. https://doi.org/10.1097/HP.0b013e318/db9eec.
Kreuzer, M., Brachner, A., Lehmann, F., Martignoni, K., Wichmann, H., Grosche, B., 2002. Characteristics of the German uranium miners cohort study. Health Phys. 83 (1), 26–34. https://doi.org/10.1097/00004032-200207000-00003.
Kreuzer, M., Walsh, L., Schnelzer, M., Tschense, A., Grosche, B., 2008. Radon and risk of extrapulmonary cancers: results of the German uranium miners' cohort study, 1960–2003. Br. J. Cancer 99 (11), 1946–1953. https://doi.org/10.1038/sj.bjc.6604776.
Kreuzer, M., Schnelzer, M., Tschense, A., Walsh, L., Grosche, B., 2010. Cohort profile: the German uranium miners cohort study (WISMUT cohort), 1946–2003. Int. J. Epidemiol. 39 (4), 980–987. https://doi.org/10.1093/ije/dyp216.
Kwon, T., Chung, Y., Yoo, J., Ha, W., Cho, M., 2020. Uncertainty quantification of bioassay functions for the internal dosimetry of radioiodine. J. Radiat. Res. 61 (6), 860–870. https://doi.org/10.1093/jrr/rraa081.
Lanzante, J.R., 2021. Testing for differences between two distributions in the presence of serial correlation using the Kolmogorov-Smirnov and Kuiper's tests. Int. J. Climatol. 1–10. https://doi.org/10.1012/joc.7196.
Leggett, R.W., Eckerman, K.F., 2001. A systemic biokinetic model for polonium. Sci. Total Environ. 275 (1–3), 109–125. https://doi.org/10.1016/S0048-9697(00)00858-5.
Li, S., Liu, X., Wang, J., Zheng, Y., Deng, S., 2019. Experimental reduced scale-study on the resistance characteristics of the ventilation system of a utility tunnel under different pipeline layouts. Tunn. Undergr. Space Technol. 90, 131–143. https://doi.org/10.1016/j.tust.2019.04.021.
Lubin, J.H., Boice, J.D., Edling, C., Hornung, R.W., Howe, G.R., Kunz, E., Kusiak, R.A., Morrison, H.I., Radford, E.P., Samet, J.M., Tirmarche, M., Woodward, A., Yao, S.X., Pierce, D.A., 1995. Lung cancer in radon-exposed miners and estimation of risk from indoor exposure. J. Natl. Cancer Inst. 87 (11), 817–827. https://doi.org/10.1093/jnci/87.11.81.
Luong, A., 2018. Asymptotic results for goodness-of-fit tests using a class of generalized spacing methods with estimated parameters. Open J. Stat. 8, 731–746. https://doi.org/10.4236/ojs.2018.84048.
Makumbi, T., Breustedt, B., Raskob, W., 2024a. Parameter uncertainty analysis of the equivalent lung dose coefficient for the intake of radon in mines: a review. J. Environ. Radioact. 276 (1–4), 107446. https://doi.org/10.1016/j.jenvrad.2024.107446.
Makumbi, T., Breustedt, B., Raskob, W., Ottenburger, S.S., 2024b. Application of INTDOSKIT tool for assessment of uncertainties on dose coefficients for ingestion of uranium by workers. Radiat. Phys. Chem. 226 (1), 112247. https://doi.org/10.1016/j.radphyschem.2024.112247.
Marsh, J.W., Bailey, M.R., 2013. A review of lung-to-blood absorption rates for radon progeny. Radiat. Protect. Dosim. 157 (4), 499–514. https://doi.org/10.1093/rpd/nct179.
Marsh, J.W., Birchall, A., 2000. Sensitivity analysis of the weighted equivalent lung dose per unit exposure from radon progeny. Radiat. Protect. Dosim. 87 (3), 167–178. https://doi.org/10.1093/oxfordjournals.rpd.a032993.
Marsh, J.W., Birchall, A., 2009. Uncertainty analysis of the absorbed dose to regions of the lung per unit exposure to radon progeny in a mine. Health Protection Agency Report. ISBN 978-0-85951-642-6. https://assets.publishing.service.gov.uk/media/5a7cfc10ed915d28e9f395a1/HPA-RPD-054_for_website.pdf.
Marsh, J.W., Bessa, Y., Birchall, A., Blanchardon, E., Hofmann, W., Noßke, D., Tomasek, L., 2008. Dosimetric models used in the Alpha-Risk project to quantify exposure of uranium miners to radon gas and its progeny. Radiat. Protect. Dosim. 1–6. https://doi.org/10.1093/rpd/ncn119.
Marsh, J.W., Blanchardon, E., Gregoratto, D., Hofmann, W., Karcher, K., Noßke, D., Tomasek, L., 2012. Dosimetric calculations for uranium miners for epidemiological studies. Radiation Protection Dosimetry, pp. 1–13. https://doi.org/10.1093/rpd/ncr310.
Martinez, M.N., Bartholomew, M.J., 2017. What does it mean? A review of interpreting and calculating different types of means and standard deviations. Pharmaceutics 9 (14), 1–23. https://doi.org/10.3390/pharmaceutics9020014.
Mbaji, R.M., Benedict, T.J., Kevin, O.O., 2023. Determinants of estimate difference between geometric measure and standard deviation. Asian J Prob. Stat. 24 (4), 23–34. https://doi.org/10.9734/AJPAS/2023/v24i4532.
Moody, J.C., Stradling, G.N., Pearce, M.J., Gray, S.A., 1994. Biokinetics of Thorium and Daughter Radionuclides After Deposition in the Rat Lung as Nitrate: Implications for Human Exposure (NRPB-M525). National Radiological Protection Board.
Nachar, N., 2008. The Mann-Whitney U: a test for assessing whether two independent samples come from the same distribution. Tutorials for Qualitative Methods for Psychology 4 (1), 13–20. https://doi.org/10.20982/tqmp.04.1.p013.
Osmanlioglu, A.E., 2022. Uranium mining techniques and waste management. Eur. J. Sustain. Dev. Res. 6 (4), 1–4. https://doi.org/10.21601/ejosdr/12273.
Papenfuß, F., Maier, A., Sternkopf, S., Fournier, C., Kraft, G., Friedrich, T., 2023. Radon progeny measurements in a ventilated filter system to study respiratory-supported exposure. Sci. Rep. 13, 10792. https://doi.org/10.1038/s41598-023-37697-7.
Paquet, F., Bailey, M.R., Leggett, R.W., Harrison, J.D., 2016. Assessment and interpretation of internal doses: uncertainty and variability. Ann. ICRP 45 (1), 202–214. https://doi.org/10.1177/0146645316633595.
Puncher, M., Harrison, J.D., 2012. Uncertainty analysis of doses from ingestion of plutonium and americium. Radiat. Protect. Dosim. 148 (3), 284–296. https://doi.org/10.1093/rpd/ncr032.
https://www.radonorm.eu. (Accessed 15 February 2025).
Rana, R., Singhal, R., 2015. Chi-square test and its application in hypothesis testing. J. Practice Cardiovascular Sci. 1 (1), 69–71. https://doi.org/10.4103/2395-5414.157577.
Romano, S., Caresana, M., Curioni, A., Silari, M., 2019. RaDoM2: an improved radon dosimeter. J. Instrum. 14 (10), P10019. https://doi.org/10.1088/1748-0221/14/10/P10019.
Samet, J.M., Hornung, R.W., 1990. Radon and lung cancer risk. Risk Anal. 10 (1), 65–75. https://doi.org/10.1111/j.1539-6924.1990.tb01021.x.
Schober, P., Vetter, T., 2020. Non-parametric statistical methods in medical research. Anesth. Analg. 131 (6), 1862–1863. https://doi.org/10.1213/ANE.0000000000005101.
Skubacz, K., Woloszczuk, K., Grygier, A., Samolej, K., 2023. Influence of dose conversion factors and unattached fractions on radon risk assessment in operating and show underground mines. Int. J. Environ. Res. Publ. Health 20, 5482. https://doi.org/10.3390/ijerph20085482.
Surucu, B., 2008. A power comparison and simulation study of goodness-of-fit tests. Comput. Math. Appl. 56, 1617–1625. https://doi.org/10.1016/j.camwa.2008.03.010.
Tai, K.Y., Dhaliwal, J., Balasubramaniam, V., 2022. Leveraging Mann-Whitney U test on large scale genetic variation data for analysing malaria genetic markers. Malar. J. 21 (79), 1–13. https://doi.org/10.1186/s12936-022-04104-x.
Vogel, R.M., 2020. The geometric mean? Commun. Stat. Theor. Methods. https://doi.org/10.1080/03610926.2020.1743313.
West, R.M., 2021. Best practices in statistics: Use the Welch t-test when testing the difference between two groups. Annals of Clinical Biochemistry 58 (4), 267–269. https://doi.org/10.1177/0004563221992088.
Widodo, N.P., Rhaditya, L.A., Purba, D.A., Waly, F.Z., Ihsan, A., Cheng, J., Syachran, S. R., Fadillah, T., Khamidah, H.N., 2023. Analysis of ventilation heat control in cut and fill underground mine working area. Paper Presented at the International Symposium on Earth Science and Technology 2023, Fukuoka, Japan. https://www.researchgate.net/publication/376413854.
https://www.radonorm.eu/workpackages/wp3-tasks/. (Accessed 20 February 2025).